

Establishment of an *in vitro* system to screen for substances to improve osteogenesis imperfecta
osteoblasts' functions



A Dissertation Submitted in Partial Fulfillment of the Requirements
for the Degree of Doctor of Philosophy in Biomedical Sciences

Inter-Department of Biomedical Sciences

Graduate School

Chulalongkorn University

Academic Year 2018

Copyright of Chulalongkorn University

การสร้างระบบทดสอบในหลอดทดลองสำหรับคัดกรองสารที่สามารถเพิ่มการทำงานของเซลล์
สร้างกระดูกของผู้ป่วยโรคกระดูกพรุนพันธุกรรม



วิทยานิพนธ์นี้เป็นส่วนหนึ่งของการศึกษาตามหลักสูตรปริญญาวิทยาศาสตรดุษฎีบัณฑิต
สาขาวิชาชีวเวชศาสตร์ สหสาขาวิชาชีวเวชศาสตร์
บัณฑิตวิทยาลัย จุฬาลงกรณ์มหาวิทยาลัย
ปีการศึกษา 2561
ลิขสิทธิ์ของจุฬาลงกรณ์มหาวิทยาลัย

Thesis Title	Establishment of an <i>in vitro</i> system to screen for substances to improve osteogenesis imperfecta osteoblasts' functions
By	Miss Wandee Udomchaiprasertkul
Field of Study	Biomedical Sciences
Thesis Advisor	Professor VORASUK SHOTELERSUK, M.D.
Thesis Co Advisor	Professor KANYA SUPHAPEETIPORN, M.D., Ph.D.

Accepted by the Graduate School, Chulalongkorn University in Partial Fulfillment of the Requirement for the Doctor of Philosophy

..... Dean of the Graduate School
(Associate Professor THUMNOON NHUJAK, Ph.D.)

DISSERTATION COMMITTEE

..... Chairman
(Professor APIWAT MUTIRANGURA, M.D., Ph.D.)

..... Thesis Advisor
(Professor VORASUK SHOTELERSUK, M.D.)

..... Thesis Co-Advisor
(Professor KANYA SUPHAPEETIPORN, M.D., Ph.D.)

..... Examiner
(Professor Sittisak Honsawek, M.D., Ph.D.)

..... Examiner
(PRASIT PHOWTHONGKUM, M.D.)

..... External Examiner
(Chulaluck Kuptanon, M.D.)

วันดี อุดมชัยประเสริฐกุล : การสร้างระบบทดสอบในหลอดทดลองสำหรับคัดกรองสารที่สามารถเพิ่มการทำงานของเซลล์สร้างกระดูกของผู้ป่วยโรคกระดูกพรุนพันธุกรรม. (Establishment of an *in vitro* system to screen for substances to improve osteogenesis imperfecta osteoblasts' functions) อ.ที่ปรึกษาหลัก : ศ. นพ.วรศักดิ์ โชติเลอศักดิ์, อ.ที่ปรึกษาร่วม : ศ. ดร. พญ.กัญญา ศุภปิติพร

โรคกระดูกเปราะพันธุกรรมเป็นโรคทางพันธุกรรมซึ่งมักจะเกิดจากการถ่ายทอดแบบยีนเด่น โดยมีสาเหตุจากการกลายพันธุ์ของยีนที่สร้างคอลลาเจนชนิดที่ 1 คือ ยีน *COL1A1* และ *COL1A2* อย่างไรก็ตามจากการศึกษาความสัมพันธ์ระหว่างจีโนไทป์และลักษณะการแสดงออกของฟีโนไทป์ยังมีความไม่สอดคล้องกันอยู่ซึ่งทำให้ยากต่อการวินิจฉัยและคาดการณ์ลักษณะทางคลินิกของผู้ป่วย คณะผู้วิจัยได้พบครอบครัวผู้ป่วยโรคกระดูกเปราะพันธุกรรมซึ่งเกิดจากการกลายพันธุ์ของยีน *COL1A2* แบบโฮโมไซกัส โดยลูกมีอาการของโรคกระดูกเปราะพันธุกรรมและฟันผุผิดปกติ ส่วนพ่อและแม่มีการกลายพันธุ์ของยีน *COL1A2* แบบเฮเทอโรไซกัส มีอาการของฟันผุผิดปกติอย่างเฉียบพลันและไม่มีประวัติกระดูกหัก ซึ่งครอบครัวนี้ถือเป็นตัวอย่างหนึ่งของความไม่สอดคล้องกันระหว่างจีโนไทป์และลักษณะการแสดงออกของฟีโนไทป์ เป็นโอกาสให้ศึกษาถึงสารทางชีวเคมีที่เป็นองค์ประกอบของการสร้างกระดูกที่น่าจะแตกต่างกันระหว่างลูกที่มีอาการกระดูกหักและพ่อแม่ที่ไม่มีอาการกระดูกหักแต่มีอาการฟันผุผิดปกติเหมือนกัน สารชีวเคมีนี้อาจจะใช้สำหรับพัฒนาการสร้างกระดูกได้ในอนาคต ดังนั้นการศึกษานี้จึงสร้างเซลล์ไอพีเอสจากครอบครัวนี้ และนำมาใช้เป็นระบบทดสอบในหลอดทดลองเพื่อค้นหาสารชีวเคมีดังกล่าวในระหว่างเจริญของเซลล์สร้างกระดูก จากผลการศึกษาการแสดงออกของยีนที่เกี่ยวข้องกับการเจริญเป็นเซลล์กระดูกคือ *COL1A1*, *COL1A2*, *SPPI*, *OCN*, *ALP* พบว่าในระหว่างการเจริญไปเป็นเซลล์สร้างกระดูก เซลล์ของลูกมีการแสดงออกของยีน *COL1A1*, *COL1A2*, *SPPI*, *OCN*, *ALP* ผิดปกติเมื่อเทียบกับพ่อแม่และตัวอย่างควบคุม โดยเฉพาะยีน *SPPI*, *OCN* ซึ่งสอดคล้องกับระดับของ osteopontin และ osteocalcin พบว่าลูกแทบไม่มีการแสดงออกเลย นอกจากนี้ยังพบความผิดปกติของการเกิดแคลเซียมในระหว่างการเจริญเป็นเซลล์สร้างกระดูกอีกด้วย การศึกษานี้สรุปได้ว่า เซลล์ไอพีเอสที่สร้างจากครอบครัวนี้ สามารถใช้เป็นระบบทดสอบในหลอดทดลองเพื่อศึกษาการเจริญของเซลล์กระดูก ซึ่ง osteocalcin และ osteopontin อาจจะเป็นสารชีวเคมีที่ใช้สำหรับพัฒนาการสร้างเซลล์กระดูกได้

สาขาวิชา ชีวเวชศาสตร์
ปีการศึกษา 2561

ลายมือชื่อนิติดี
ลายมือชื่อ อ.ที่ปรึกษาหลัก
ลายมือชื่อ อ.ที่ปรึกษาร่วม

5887802520 : MAJOR BIOMEDICAL SCIENCES

KEYWORD: Osteogenesis imperfecta, COL1A2 mutation, induced pluripotent stem cells, osteogenic markers, osteoblast differentiation

Wandee Udomchaiprasertkul : Establishment of an *in vitro* system to screen for substances to improve osteogenesis imperfecta osteoblasts' functions. Advisor: Prof. VORASUK SHOTELERSUK, M.D. Co-advisor: Prof. KANYA SUPHAPEETIPORN, M.D., Ph.D.

Background: Osteogenesis imperfecta (OI) is a heritable bone disorder caused mainly by dominant mutations in genes encoding collagen-related proteins which are *COL1A1* and *COL1A2*. Genotype-phenotype correlation has some discrepancies which lead to the difficult prediction of the clinical outcome of OI patients. We identified a child with dentinogenesis imperfecta (DI) and OI who was homozygous for c.1009G>A (p.G337S) mutation in *COL1A2*. Her parents were heterozygous for the mutation and had only DI. This family provides the opportunity to explore the biochemical changes which are different between the homozygous with DI and OI and the heterozygous with DI only. Methods: We established patients-specific induced pluripotent stem cells (iPSCs) from the trio to use as an *in vitro* system to screen for biochemical substances. They were used to study the expression of the osteogenic marker genes (*COL1A1*, *COL1A2*, *SPP1*, *OCN*, *ALP*) and their products along the time course of osteoblast differentiation. Results: We successfully generated patient-specific iPSCs from the trio. They all showed the characteristic features of iPSCs. We then differentiated them to mesenchymal stem cells (MSCs) and osteoblasts. Their osteoblasts showed various defective expression of the osteogenic markers and calcium mineralization. Interestingly, osteopontin was absent in iPSCs-derived osteoblasts of patients with OI, while it was significantly lower in those with DI-only compared to an unaffected control. In addition, osteocalcin was significantly lower in those with OI compared to DI-only and an unaffected control. Conclusion: Levels of osteopontin and osteocalcin in iPSCs-derived MSC of patients with OI were significantly low during osteoblasts differentiation. These cells could be used to screen for substances which can increase osteopontin and osteocalcin.

Field of Study: Biomedical Sciences

Student's Signature

Academic Year: 2018

Advisor's Signature

Co-advisor's Signature

ACKNOWLEDGEMENTS

I would like to thank HRH Princess Chulabhorn College of Medical Science, Chulabhorn Royal Academy for giving me the opportunity to being a student here and providing the funding for the study. A very special gratitude goes out to all down at by the Thailand Research Fund and the Chulalongkorn Academic Advancement into Its 2nd Century Project for providing the funding for the work. I would like to express my sincere gratitude to my thesis advisor, Prof. Vorasuk Shotelersuk for his invaluable advice. I am most grateful for his teaching and endless inspiration as well as giving me a good positive mindset in life and at work, without his supervision, it would not be impossible to complete my thesis. I am very thankful to Prof.Kanya Suphapeetiporn for her advice and constant encouragement throughout the course. In addition, I am grateful to Dr.Ruttachuk Rungsiwiat and his team for teaching and invaluable helping me in the part of stem cell technology. It was fantastic to have the opportunity to work majority of my research in his facilities. I would also like to thank the member of Excellence Center for Medical Genetics, King Chulalongkorn Memorial Hospital including Mr. Chalurmpon Srichomthong, Dr. Rungnapa Ittiwut, Dr. Chureerat Phokaew, Dr. Chupong Ittiwut, Miss. Nalinee Hemwong, Miss. Kanyanut Thaweerachatham, and others person who helps me by providing their valuable assistance and time, especially to Miss Siraprapha Tongkobetch for always listening and assisting as well as giving me the valuable suggestion. I am also grateful to the staffs of Stem cell and cell therapy research center, Faculty of Medicine, Chulalongkorn University for assisting and providing time to my work. I would also like to thank my friend, Miss Thivaratana Sinthuwiwat for encouragement and for pushing me further than I thought I could go. Most of all, I am fully indebted to Mr.Thoranin Intarajak for his understanding, wisdom, patience, enthusiasm, and well take care of me throughout the study. Finally, I most gratefully acknowledge my family and my friends for all their support throughout the period of this research. I would not have achieved this far, and this thesis would not have been completed without all the support that I have always received from them.

Wandee Udomchaiprasertkul

TABLE OF CONTENTS

	Page
ABSTRACT (THAI).....	iii
ABSTRACT (ENGLISH).....	iv
ACKNOWLEDGEMENTS.....	v
TABLE OF CONTENTS.....	vi
List of figures.....	1
List of tables.....	3
Background and rationale.....	4
Review of related literature.....	7
Osteogenesis imperfect.....	7
Type of OI.....	9
Genotype-phenotype correlation.....	10
Osteoblast differentiation and bone formation.....	10
Type I collagen biosynthesis.....	13
Research questions.....	20
Hypothesis.....	20
Objectives.....	20
Conceptual framework.....	21
Research methodology.....	22
1. Participants.....	22
2. Mutation analysis.....	23
3. Generation of patient-specific iPSCs.....	24

4. Characterization of patient-specific iPSCs.....	26
5. Generation of iPSCs-derived MSCs.....	29
6. Investigation of the pathways involving osteoblast differentiation	30
7. Type I collagen detection	30
8. Investigation of biochemical substances involving mineralization.....	31
Results.....	34
1. Clinical data.....	34
2. Generation of patients-specific iPSCs.....	40
3. Characterization of patient-specific iPSCs.....	42
4. Generation of iPSCs-derived MSCs.....	46
5. Flow cytometry analysis.....	47
6. Karyotype analysis	48
7. Investigation of type I collagen synthesis and overmodification.....	49
8. Investigation of osteogenic gene expression involving osteoblast differentiation.....	51
9. Investigation of biochemical substances involving mineralization.....	58
Discussion.....	60
REFERENCES	65
Appendix.....	70
VITA	74

List of figures

	Page
Figure 1 Type of OI.....	9
Figure 2 A lists of differentiation marker for MSCs, pre-osteoblasts, osteoblasts, and osteocytes during MSC differentiation to osteoblasts and osteocytes	11
Figure 3 Structure of type I procollagen.....	15
Figure 4 The schematic diagram showing the different posttranslational modifications and assembly of type I collagen into fibrils.....	16
Figure 5 The extracellular matrix disease paradigm.....	18
Figure 6 The family's pedigree of proband.....	22
Figure 7 Generation of iPSCs from dermal fibroblast by episomal transfection.	25
Figure 8 Clinical features associated with proband.....	35
Figure 9 Clinical features associated with mother and father of proband.....	36
Figure 10 Mutation analysis of trio.	39
Figure 11 The established iPSC of proband.....	41
Figure 12 Expression of pluripotent transcription factor.....	42
Figure 13 Immunocytochemical staining of pluripotent markers.....	43
Figure 14 Immunocytochemical staining of three-germ layer markers.	44
Figure 15 Electrochromatogram of the mutation in exon 19 and 44 of <i>COL1A2</i> gene.....	45
Figure 16 Morphology of proband iPSC-derived MSC.	46
Figure 17 Karyotype analysis of iPSC-derived MSC.	48
Figure 18 Collagen I secreted from MSC-derived osteoblast.....	49
Figure 19 Level of procollagen I propeptide (PIP).	50
Figure 20 Expression of <i>COL1A1</i> gene.....	52

Figure 21 Expression of <i>COL1A2</i> gene.....	53
Figure 22 Expression of <i>SPP1</i> (OPN) gene.	54
Figure 23 Expression of <i>OC</i> gene.....	55
Figure 24 Expression of <i>ALP</i> gene.....	56
Figure 25 Calcium deposit during osteoblast differentiation.	57
Figure 26 Level of extracellular osteocalcin.	58
Figure 27 Level of extracellular osteopontin.....	59



List of tables

	Page
Table 1 Genetics classification of osteogenesis imperfecta.....	8
Table 2 Primers for PCR and sequencing	27
Table 3 Primary and secondary antibodies used in immunofluorescence assay	28
Table 4 Probes for real-time PCR	32
Table 5 Filtering criteria for the exome sequencing of proband	37
Table 6 Filtering criteria for the exome sequencing of pt (FII)	38
Table 7 Number of established patient-specific iPSC cell line from all participants	40
Table 8 Level of surface marker expressed on iPSC-derived MSC	47
Table 9 Raw data of total protein quantitated by BCA assay	70
Table 10 Level of osteocalcin/total protein (ng/mg)	70
Table 11 Level of osteocalcin/total protein (ng/mg)	71
Table 12 Level of PIP/total protein (ng/mg)	71
Table 13 Raw quantitative qPCR cycle threshold for osteogenic genes and housekeeping gene.....	72

Background and rationale

Osteogenesis imperfecta (OI) or brittle disease is a rare heritable disease characterized by bone fragility, bone deformity, and growth retardation which associated dentinogenesis imperfecta (DI), blue sclerae, conductive or sensory hearing loss, pulmonary function impairment, malocclusion, muscle weakness, and ligamentous laxity (1). In its classical and more common forms, OI is caused by dominant mutations in either of gene encoding type I collagen, *COL1A1* and *COL1A2*. An individual with OI do not appropriately develop bone mass; therefore, they have a high chance to bone fracture. Glycine substitution in the helical domain of *COL1A1* and *COL1A2* lead to misfolded and over-modification of type I procollagen result in the qualitative defect of type I collagen in OI (2). Normally, abnormal type I collagen is degraded, however; some abnormal type I collagen secreted and incorporated into the extracellular matrix. The gold standard of the diagnosis of OI is the BMD measurement. However, the limitation of BMD measurement including the difficult to identify the outline of the bone of OI patient and limit the time of the BMD measurement per year resulting in the difficult to diagnosis and monitor the response after the treatment (3).

Low level of type I collagen and incorporate of abnormal type I collagen in extracellular matrix leads to a failure to alter specific transcription factor expression and maintain the osteoblast differentiation program in OI osteoblast. Several osteogenic markers responsible for the bone formation are stimulated by the key transcription factor that is *RUNX2*. *RUNX2* stimulates the expression of *OCN*, *BSPH*, *ALP*, and *OPN* through MAPK kinase pathway. These genes encoded for bone matrix components of the bone, for example; osteocalcin, bone sialoprotein II, alkaline phosphatase, osteopontin, and type I collagen, which differentially expresses during bone development by osteoblast. The low expression of osteoblast-specific genes, for example; *OCN*, *ALP*, *SPARC*, and *COL1A1* have been reported in OI (4, 5). The explanation of this situation is ER stress response of the osteoblast to abnormal type I collagen lead to deficient osteoblast differentiation and maturation. The decrease of ER dilation in OI osteoblast by rapamycin treatment partially rescued osteoblast maturation and mineral deposition (5). The second possibility is a defect in the interaction between the extracellular matrix and transmembrane adhesion molecule of osteoblast, which subsequently interferes signal

transduction pathway including the MAPK kinase pathway. Therefore, there is the possibility to induce RUNX2 activity or decrease ER stress in OI osteoblast, which results in enhancing the expression of osteogenic markers and subsequently increases the bone matrix. The set up of an in vitro system to monitor osteoblast function may provide the opportunity to screen for substances to improve osteoblast function in OI patients.

Normally, osteoblast originates from a mesenchymal stem cell (MSC) that compose of three stages of differentiation; proliferation, matrix production/maturation, and mineralization. The use of iPSC as a disease modeling has advantages which are an unlimited resource for exploring pathogenesis and for investigating the therapeutic treatment that provides a genetic signature of human tissue. Furthermore, iPSC is capable of differentiating into MSC, and then osteoprogenitor. It allows accessing the transition from osteoprogenitor into the osteoblast. Therefore, the expression of osteogenic markers during osteoblast differentiation is definitely explored and used for evaluating the association between osteogenic markers expression and bone fracture among OI patients. The present study will establish patient-specific iPSC of OI type III patients with a homozygous p.G337S COL1A2 mutation and her heterozygous parents who display only DI, lack of sign and symptoms of skeletal fragility. It is noteworthy that this mutation has been reported as autosomal dominant inheritance, however; it is inherited by autosomal recessive manner for this family. Moreover, there is a few reports about bi-allelic COL1A2 mutation in OI (6), (7). This family provides the opportunity to explore the biochemical substance involving bone development pathway that related to bone fracture susceptibility of OI patients with the same genetic background. Besides, an unrelated boy with OI type I who carries heterozygous p.G961D COL1A2 mutation will be explored in this work.

Taken together, this study aims to establish the patient-specific iPSC to use as an in vitro system for exploring the biochemical substance to improve OI osteoblast function. In addition, this system will be used for investigating the biochemical substances in particular of bone formation markers and also their level that related to fracture susceptibility of OI patients. Biochemical substances may be used as a surrogate marker for bone fracture susceptibility and for evaluation of medical treatment. Base on the previous report, an in vitro system will be used for monitoring the improvement of osteoblast function by either targeting at RUNX2 or decrease ER dilation by treat with the validated substance in the further study. It will be expected that

osteoblast function may be rescued and showed the increase in the biochemical substance related to fracture susceptibility of OI patient to a nearly normal level. According to the present study, the aim is improving the level of biochemical substance related to bone fracture susceptibility of OI type III patient to close to that of her parents. Moreover, the biochemical substance related to fracture susceptibility of OI patient may be used in the diagnosis and monitor the treatment in OI patient.



Review of related literature

Osteogenesis imperfect

Osteogenesis imperfect (OI) is a brittle bone disease which is mainly caused by the autosomal dominant mutations of the gene encoding for type I collagen (*COL1A1* and *COL1A2*). The birth prevalence of OI in Europe and the United States is about 0.3-0.7 per 10,000 births. Most patients are the heterozygous mutation in either *COL1A1* or *COL1A2* have been well established to cause OI type I, II, III or IV. In addition, mutation in several genes involved in type I collagen biosynthesis, processing, post-translational modification, and altered bone cell differentiation which responsible for recessive, dominant, and X-linked OI have been founded; for example, *IFITM5*, *P3H1*, *MBTPS2*, *BMP1*, *PLOD2*, *CREB3L1*, *SP7*, *SPARC*, *CRTAP* and *WNT1* (Table 1). Mutation in these genes is identified as a cause of OI type V-XVIII (8). OI is characterized by a spectrum of susceptibility to fractures of the long bones and vertebral compressions, variable deformity of long bones, ribs, spine, and substantial growth deficiency due to low bone mass, whose often exhibit dentinogenesis imperfecta, blue sclerae, hearing loss, decreased pulmonary function, and cardiac valvular regurgitation (8).

Table 1 Genetics classification of osteogenesis imperfecta (2)

Mutated gene	Encoded protein	Osteogenesis imperfecta type based on the genetic classification	Inheritance	OMIM	Clinical characteristics
Impairment of collagen synthesis and structure					
COL1A1 or COL1A2	Collagen α 1(I) (COL1A1) or α 2(I) (COL1A2)	I, II, III or IV*	AD	• 166200 • 166210 • 259420 • 166220	Classic phenotype (see BOX 1)
Compromised bone mineralization					
IFITM5	Bone-restricted interferon-induced transmembrane protein-like protein (BRIL; also known as IFM5)	V	AD	610967	Normal-to-severe skeletal deformity, intraosseous membrane ossifications, radiodense band and radial head dislocation, normal-to-blue sclerae and sometimes hearing loss
SERPINF1	Pigment epithelium-derived factor (PEDF)	VI	AR	613982	Moderate-to-severe skeletal deformity, the presence of osteoid, fish-scale appearance of lamellar bone pattern and childhood onset
Abnormal collagen post-translational modification					
CRTAP	Cartilage-associated protein (CRTAP)	VII	AR	610682	Severe rhizomelia with white sclerae
P3H1 (previously known as LEPRE1)	Prolyl 3-hydroxylase 1 (P3H1)	VIII	AR	610915	
PPIB	Peptidyl-prolyl <i>cis</i> - <i>trans</i> isomerase B (PPIase B)	IX	AR	259440	Severe bone deformity with grey sclerae
Compromised collagen processing and crosslinking					
SERPINH1	Serpin H1 (also known as HSP47)	X	AR	613848	Severe skeletal deformity, blue sclerae, dentinogenesis imperfecta, skin abnormalities and inguinal hernia
FKBP10	65 kDa FK506-binding protein (FKBP65)	XI	AR	610968	Mild-to-severe skeletal deformity, normal-to-grey sclerae and congenital contractures
PLOD2	Lysyl hydroxylase 2 (LH2)	No type	AR	609220	Moderate-to-severe skeletal deformities and progressive joint contractures
BMP1	Bone morphogenetic protein 1 (BMP1)	XII	AR	614856	Mild-to-severe skeletal deformity and umbilical hernia
Altered osteoblast differentiation and function					
SP7	Transcription factor SP7 (also known as osterix)	XIII	AR	613849	Severe skeletal deformity with delayed tooth eruption and facial hypoplasia
TMEM38B	Trimeric intracellular cation channel type B (TRIC-B; also known as TM38B)	XIV	AR	615066	Severe bone deformity with normal-to-blue sclerae
WNT1	Proto-oncogene Wnt-1 (WNT1)	XV	• AR • AD	• 615220 • Unknown	Severe skeletal abnormalities, white sclerae and possible neurological defects
CREB3L1	Old astrocyte specifically induced substance (OASIS; also known as CR3L1)	XVI	AR	616229	Severe bone deformities
SPARC	SPARC (also known as osteonectin)	XVII	AR	616507	Progressive severe bone fragility
MBTPS2	Membrane-bound transcription factor site-2 protease (S2P)	XVIII	XR	Unknown	Moderate-to-severe skeletal deformity, light blue sclerae, scoliosis and pectoral deformities

AD, autosomal dominant; AR, autosomal recessive; OMIM, Online Mendelian Inheritance in Men (OMIM) database (<http://www.omim.org>); XR, X-linked recessive

*Classical types of OI

Type of OI

The classification of OI proposed by Sillence et al in 1979 has been categorized into type I-IV (Figure 1) based on clinical presentation, radiographic features, and patterns of inheritance. They are caused by an autosomal dominant mutation in COL1A1 and COL1A2 gene (8).

OI Type I is the mildest type of OI. The individuals have a minimal bone deformity, nearly normal and without DI. They have bone fractures, blue sclera, and hearing loss (1).

OI Type II is perinatally lethal form. The hallmarks of type II are shortened and deformed limbs. The most common cause of death in the first postnatal week is respiratory failure (9, 10).

OI Type III is the most severe form of non-lethal with progressive deforming. The individuals may undergo hundreds of fractures. They have triangular facies, frontal bossing, blue/grey sclerae, DI, vertebral compressions and scoliosis (1).

OI Type IV is the most variable form with ranging from mild to moderately severe. The individuals are usually shortly than average, long bone fractures, hearing impairment, white scleral and DI (1).

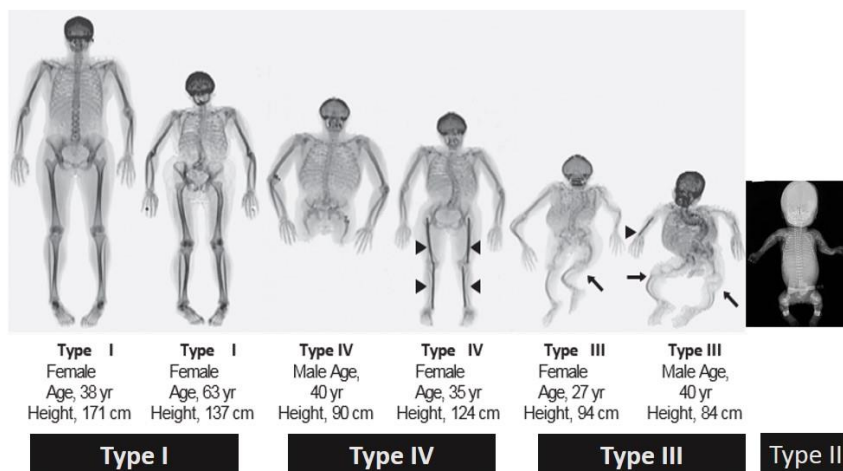


Figure 1 Type of OI (11)

Genotype-phenotype correlation

Genotype-phenotype correlation in OI caused by the mutation in helical domain of COL1A1 and COL1A2 have been investigated in the several studied (10, 12-14). These studies explored the relationship between the type of OI and specific collagen I mutated region and clinical features including the presence of dentinogenesis imperfecta and/or blue sclera to predict the clinical outcome in OI patients.

Forlino et al (2011) suggested that the molecular defect in type I OI is a null COL1A1 allele which causing decrease the synthesis of structurally normal collagen. OI type II-IV are usually caused by the deficiency of type I collagen structure, mostly glycine substitutions. The substitutions in the N-terminus of both 1(I) and 2(I) chain are non-lethal and cause a different pattern of lethality resulting from the different role in the matrix organization of each chain. Both lethal and non-lethal forms of OI due to the substitutions at over 40 glycine residues suggesting the important role of modifying factors (10).

Maioli et al (2019) investigated genotype-phenotype correlation in 364 OI type I-IV Italian patients. The studied reported the additional observation such as a new effect for 1(I) - and 2(I) -serine substitutions and the association of cardiovascular abnormalities with quantitative mutations. According to the previous studies, the presence of a COL1A2 mutation significantly affects the severe stature reduction. Interestingly, they reported the different findings of the relationship between specific collagen I mutated region and the presence of dentinogenesis imperfecta and/or blue sclera. They found that the glycine substitutions in the first 127 amino acids of 1(I) and within the first 121 amino acids of 2(I) in the triple helical domain related to the absence of dentinogenesis imperfecta. The studies indicated that the discrepancies between genotype and phenotype lead to the difficult to define the clinical outcome in OI patient (10, 12-14).

Osteoblast differentiation and bone formation

Bone is composed of an organic phase and the inorganic phase. The inorganic phase consists mainly of hydroxyapatite, which is complex of calcium and phosphate. The organic phase constituted by 90% type I collagen and 5% noncollagenous proteins such as proteoglycans, bone sialoprotein II, osteocalcin, osteopontin, osteonectin, bone morphogenetic proteins,

fibronectin, and growth factors (15) (16). Bone is constantly undergoing remodeled through the dynamic process, which is bone formation by osteoblast and bone resorption by osteoclast. Osteoblast originate from mesenchymal stem cell in the bone marrow that commits to the osteoprogenitor cell (2). During the transition of osteoprogenitor to osteoblast require the expression of *RUNX2*, *DLX5*, and *OSX*. *RUNX2* is a master regulator of osteoblast differentiation, which regulates the expression of several osteoblast genes such as *COL1A1*, *ALP*, and *OC* (Figure 2). Osteoblast synthesizes collagen proteins, mainly type I collagen, and noncollagenous proteins (osteocalcin, osteonectin, BSP, and osteopontin) as well as proteoglycan to form organic matrix followed by mineralization of bone matrix. The mineralization occurs by the deposition of hydroxyapatite crystals that generated through a localized enzymatic accumulation of calcium and phosphate ions (17).

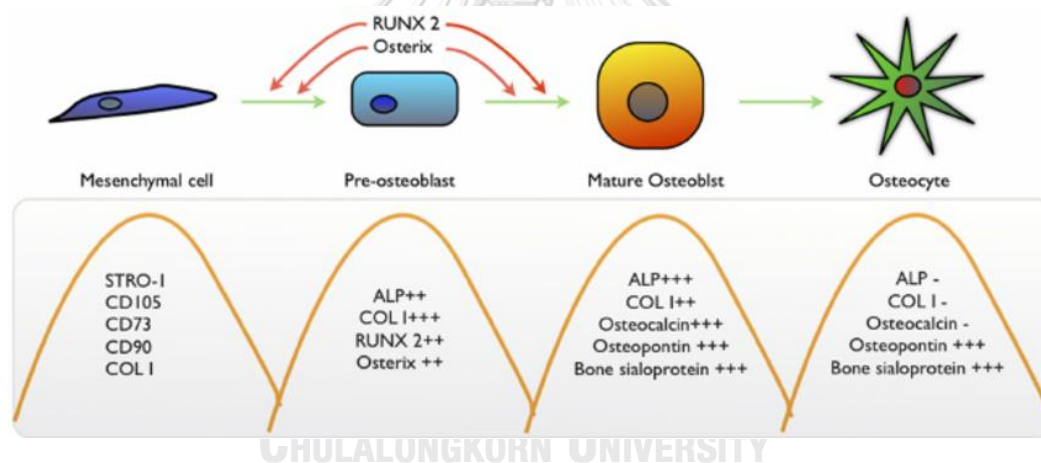


Figure 2 A lists of differentiation marker for MSCs, pre-osteoblasts, osteoblasts, and osteocytes during MSC differentiation to osteoblasts and osteocytes (18)

Alkaline phosphatase is highly expressed in both bone tissues and calcifying cartilage tissues, which have an important role in osteogenesis. *ALP* is located on the cell surface and in matrix vesicles. *ALP* expression is high in the early development process. In the late stage of development, *ALP* expression decreases while other genes (osteocalcin) are upregulated. Mineralization begins with the formation of hydroxyapatite in the matrix vesicle budding from

osteoblast. Hydroxyapatite is created from calcium and inorganic phosphate (Pi) which penetrate from matrix vesicle membrane via the activity of tissue-nonspecific alkaline phosphatase (TNAP) and then deposited between collagen fibrils. TNAP hydrolyzed inorganic pyrophosphate (PPi), which is generated by NPP1 and transported outside the cells by ANKH. PPi inhibits hydroxyapatite formation; therefore, the balance between the activities of TNAP, NPP1, and ANKH is important for hydroxyapatite formation (19).

Osteocalcin (bone gla protein) is one of the most abundant non-collagenous proteins, which is secreted by osteoblasts and odontoblasts, and it is expected to regulate bone mineralization. Besides, osteocalcin is involved in bone resorption via enhancement of the osteoclast maturation in the presence of macrophage colony-stimulating factor (M-CSF) and RANKL (20). Osteocalcin is a small protein of 49 amino acids including three glutamic residues, which undergoes carboxylation by vitamin K-dependent enzymatic carboxylation to form the gamma-carboxyglutamic acid (gla) before secretion from osteoblast. The carboxylated gla residues provide osteocalcin with the ability to bind to calcium in bone hydroxyapatite with a high affinity. In contrast, uncarboxylated osteocalcin is more likely leaked into circulation because it has low affinity to bind hydroxyapatite. Nevertheless, both the carboxylated and the noncarboxylated form of osteocalcin are released into the circulation where they can be detected that is widely used in the clinical investigation as bone formation (21, 22). Circulating osteocalcin has been widely used in clinical investigations as a marker of bone formation. In addition, circulating osteocalcin can be generated from activities associated with the bone resorption process, when osteocalcin incorporated in the bone matrix is released during bone degradation. Several studies display that the levels of circulating osteocalcin are associated with changes in the rate of bone turnover in metabolic bone diseases such as osteoporosis (23).

Osteopontin and bone sialoprotein is the member of the SIBLING (small integrin-binding ligand, N-linked glycoprotein). Osteopontin and bone sialoprotein play a role in the step of mineral formation *in vitro*; therefore, they are probably candidates responsible for bone formation (24). Osteopontin is secreted by osteoblast and is displayed as a major component of the non-collagenous bone matrix. Osteopontin mediates autocrine and paracrine functions in the regulation of tissue formation that inhibits mineralization by binding to growing hydroxyapatite

crystal via negatively charged phosphate residues (25). In addition, osteopontin is important for recruiting osteoclasts for bone remodeling. under tensile mechanical stress

Bone sialoprotein (BSP II) is synthesized by osteoblast, osteoclast, osteocyte, and hypertrophic chondrocyte. BSP II triggers hydroxyapatite formation in vitro and seems to mediate cell-cell interactions via an integrin binding site. A small amount of BSP II is found in the circulation and act as a potential marker of bone turnover (21). Mice with BSP II deficiency impairs bone growth and deposition of the mineralized matrix, which associate with dramatically reduced bone formation (26). However, the role of BSP II is not fully understood.

Type I collagen biosynthesis



Type I collagen is consisting of heterotrimer of two 1(I) chains and one 2(I) chain encoded by *COL1A1* and *COL1A2*, respectively (Figure 3). Type I collagen is synthesized in the form of procollagens with N- and C-terminal propeptide domains, which biosynthesis of procollagen occurs in ER followed by a series of a post-translational modification. Hydroxylation of specific proline residues of procollagen chains is catalyzed by prolyl-4-hydroxylases and prolyl-3-hydroxylase. While, hydroxylation of specific lysine residues is catalyzed by lysyl hydroxylases (LH1 and LH2), and can be subsequently modified by glycosylation of hydroxylysines by galactosyltransferase 1 and galactosyl hydroxylysyl-glucosyl transferase before the formation of a triple helical procollagen molecule. The triple helix formation between procollagen chains is preceded from the C-terminal end to the N-terminal end direction by folding and disulfide bond formation within the individual C- propeptides. After procollagens are transported across Golgi network, the N-terminal propeptides (PINP) and C-propeptides (PICP) are cleaved from fully folded procollagen that has short telopeptides at either end results in assembling of collagen molecules into the fibrils (8) (27). After PINP and PICP are cleaved, they are subsequently released into the ECM (Figure 4). Therefore, the level of PINP and PICP can serve as markers of type 1 collagen secretion by osteoblasts (28). The strengthening of the extracellular collagenous matrix occurs through the formation of intra- and inter-molecular crosslinks within fibrils as a result of the action of lysyl oxidase (LOX)(29).

Mutations of *COL1A1* and *COL1A2* can result in the reduction of the amount of normal type I collagen (quantitative defect) or in the synthesis of type I collagen molecule with a

structural defect (qualitative defect). The most common mutation that is glycine substitution within the Gly-X-Y repeat of the triple helix of type I collagen disturbs helix formation and linear folding, which cause a delay folding process resulting in collagen over modification of alpha chains in the helix including increased hydroxylation and glycosylation. These over modified collagen molecules assemble into abnormal fibrils, leading to the generation of the disorganized extracellular matrix (ECM). Since the role of type I collagen in the bone strength is to provide the ductility and ability to absorb energy; i.e, the toughness. The cooperation of aberrant collagen in ECM affect the mechanical properties of bone and increase fracture susceptibility, which is one of the key features of bone fragility in OI (2), (27).

Pathogenesis of OI due to mutation of *COL1A1* and *COL1A2* has been revealed by studies in an animal model such as a mouse model. In certain instances, the abnormal collagen is maintained in the ER resulting in ER stress, which has been impaired osteoblast differentiation via autophagy stimulation and apoptosis activation (2). According to the previous report, the osteoblast obtained from a mouse carrying G610C substitution in *Col1a2* exhibit cell stress response due to the retention of the misfolded collagen molecule, which causes osteoblast malfunction, decrease collagen synthesis, decreases bone mass accumulation, and then abnormal bone matrix deposition and mineralization (5).

Normally, quantitative defects of *COL1A1* expression cause OI type I or early onset osteoporosis. While qualitative defects of type I collagen take place in both 1(I) chains and 2(I) chain. The study in bone marrow mesenchymal stem cells obtained from OI type III patient with *COL1A2* mutation revealed that expression level of osteoblast-specific markers, which are *BGLAP*, *COL1A1*, *MSX2*, *SPARC*, and *VDR* during differentiation into osteoblast is lower than that of healthy control (4).

Nowadays, there is no biochemical marker for the risk of bone fracture in OI. There were several studies to investigate biochemical bone markers in a patient's sample including urine and serum. The previous study explored the level of the bone marker in OI patient type I, III and IV. It is shown that total ALP did not differ significantly between OI types. When compared with the control group, total ALP, and the B2 isoform were significantly higher in children with OI types I and IV. Moreover, osteocalcin level was significantly higher in OI type I, while the PICP level is higher in OI type IV, in comparison with the other OI types. After treatment for 1-

1.5 years, all bone marker diseased in different relative amounts. In addition, there are no significant differences in bone markers found between the age - and type - matched subgroups with or without vertebral compressions (30).

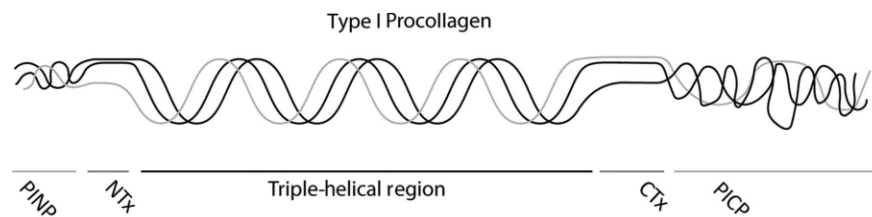


Figure 3 Structure of type I procollagen (28). Type I procollagen folded in triple helix formation. N-terminal propeptides (PINP) and C-propeptides (PICP) are cleaved from fully folded procollagen. CTX and NTX are C- and N-terminal telopeptides of type I collagen, respectively.

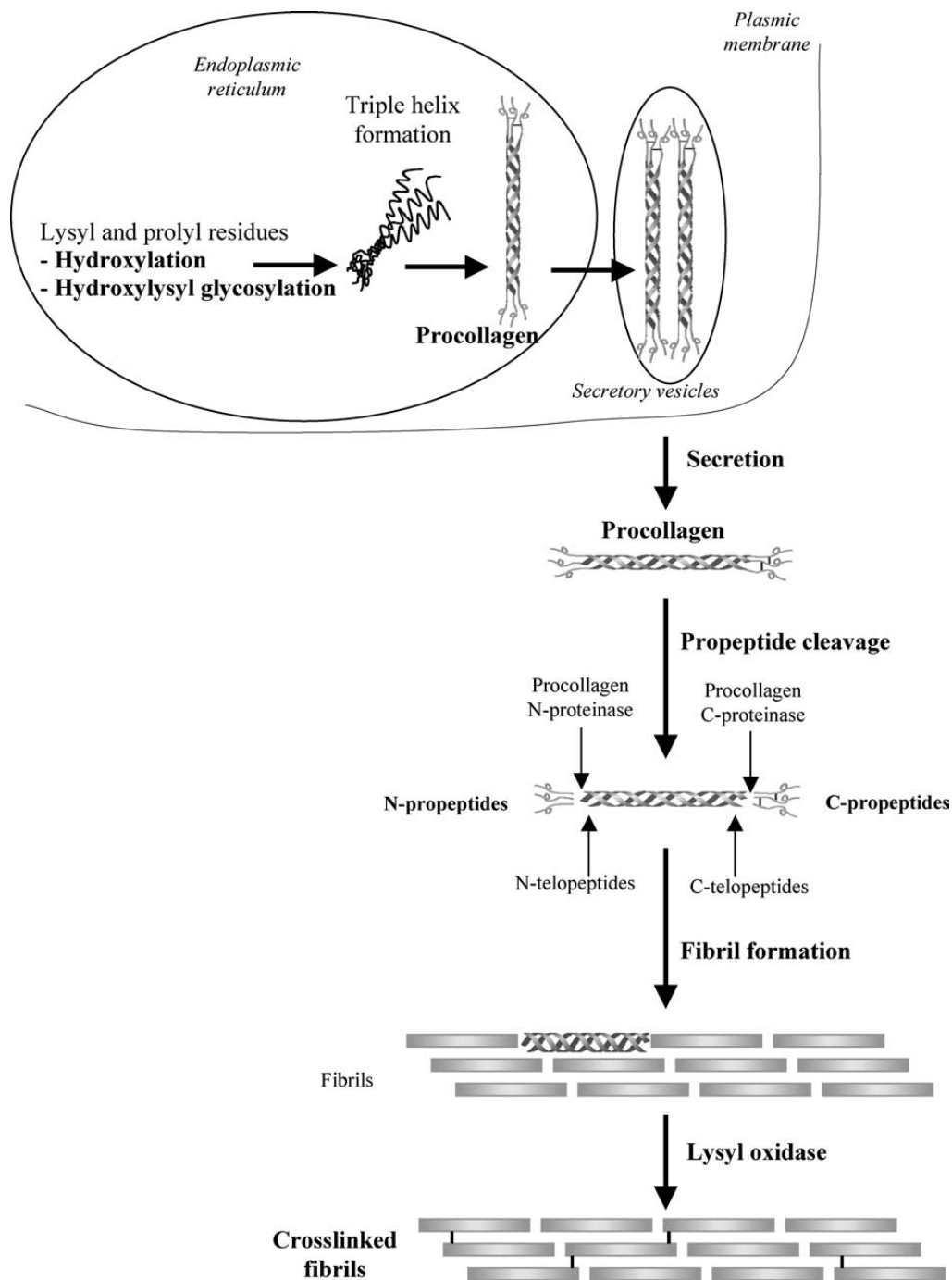


Figure 4 The schematic diagram showing the different posttranslational modifications and assembly of type I collagen into fibrils (31).

The tendency of bones to fracture depends on the bone quality, which is the presence of mineralized tissue. The degree of mineralization of the bone matrix that determined by measurements of the bone mineralization density distribution was found to be almost universally increased in OI. Consistently, the mean calcium content of bone matrix of biopsy samples obtained from children with a mild phenotype and either qualitative or quantitative *COL1A1* or *COL1A2* mutations revealed a similar level. In the patients with more severe phenotype (type IV and type III) and in recessive type VII and type VIII exhibit the same result (8).

The important mechanisms controlling cell fate and function are mediated by cell adhesion molecules including cell-cell and cell-matrix. Osteoblast expresses several kinds of integrin, however; beta1 integrin plays an important role in osteoblast differentiation. Alpha2beta1 integrin is a major receptor for type I collagen, which controls MSC osteogenic differentiation and survival through ROCK, FAK, and MAPK ERK1/2 signaling (32). Runx2 is phosphorylated and activated by the MEK/ERK branch of the MAPK pathway (33). Altered in the extracellular matrix in OI may perturbed receptor recognition of matrix components and subsequent signal transduction including the signaling pathway involving type I collagen interaction with integrin, which activates MAPK that then activate RUNX2. Reduced type I collagen in the matrix in OI may result in reduce RUNX2 activation and activity lead to failure in osteoblast differentiation. The second possible way is ER stress response to accumulated abnormal type I collagen in osteoblast, which involves upregulation of chaperones and caspases that promote cell apoptosis (Figure 5)(2). The mature osteoblasts are more likely to apoptosis in response to chronic stress. In addition, dominant effect of mutation resulted from reduced synthesis and secretion rate, or disrupt the interaction in ECM. Abnormal proteins lead to cellular retention and/or degradation of mutant protein, and normal proteins being gathered into mutant-containing multimers. The assemble of mutant proteins in ECM and ER stress response result in severe protein deficiency (2). It might be suggested that the reduction of ER dilation in OI osteoblast by rapamycin treatment partially rescued osteoblast maturation and mineral deposition (5).

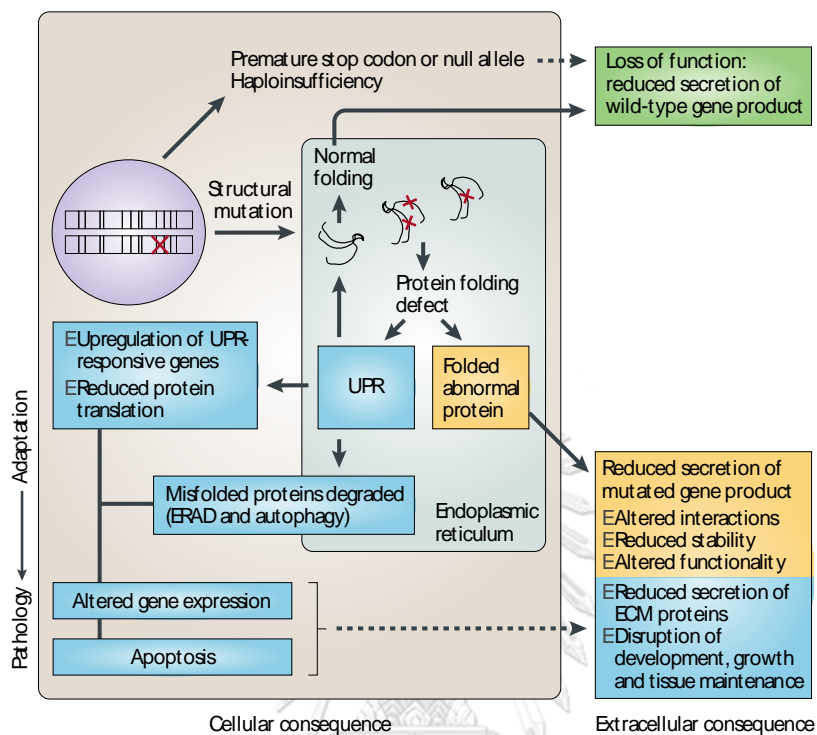


Figure 5 The extracellular matrix disease paradigm (2). Pathophysiology process of ECM mutation including the extracellular consequence and the molecular pathology.

There are several reports demonstrate the activation of RUNX2 signaling pathway through the growth factor, for example; fibroblast growth factor 2 (FGF2) and bone morphogenetic protein (BMP) (34), (33), (35), (3, 36, 37). The BMPs are secreted by osteoblast and incorporated into ECM, and then activate osteogenic genes through MAPK pathway. The report revealed that BMP2, BMP4, and BMP7 increase the expression of OCN and BSP1 mRNA. Moreover, the administration of BMP2 induced RUNX2 activity and ALP activity, as well as subsequent osteoblastic differentiation through p38 and ERK1/2 signaling (35). Besides, FGF2 stimulates OCN mRNA expression. This stimulation required RUNX2 and its DNA binding site in the osteocalcin promoter. FGF2 administration dramatically increased phosphorylation of ERK1/2 followed by phosphorylation of RUNX2 (33). Moreover, the degradation of RUNX2 occurred through the induction of MAPK-ERK signaling in TGF-beta mediated osteoblast differentiation. Inhibition of osteoblast differentiation by TGF-beta was rescued by treatment of MAPK-ERK inhibitor, U0126, lead to increase RUNX2, ALP, and OCN mRNA expression (38). According to the previous study reports that the excessive TGF-beta in OI mouse model leads to upregulated of TGF-beta signaling. Treatment with anti-TGF-beta can correct bone phenotype of OI mouse (39). These reports demonstrated the important roles of RUNX2 to regulate osteoblastic differentiation.

Therefore, this study provides the possibility to improve osteoblast function by induction of RUNX2 activity or reduction of ER stress in OI patient, both of them may rescue osteoblast differentiation and maturation leads to increase the expression of osteogenic markers and subsequently increase in bone matrix. Moreover, an in vitro system may provide the opportunity to screen for substances to improve osteoblast function in OI patients.

Key words

OI, iPSC, Osteoblast differentiation, Type I collagen synthesis

Abbreviation

OI: osteogenesis imperfecta, iPSC; induced pluripotent stem cell

Research questions

1. Can patient-specific iPSCs display characteristics of OI osteoblasts and be used as an *in vitro* system to screen for substances to improve OI osteoblasts' functions?
2. Which substances in mutant *COL1A2*, iPSC-derived osteoblast lineage cells have different levels between those with and without clinical OI?

Hypothesis

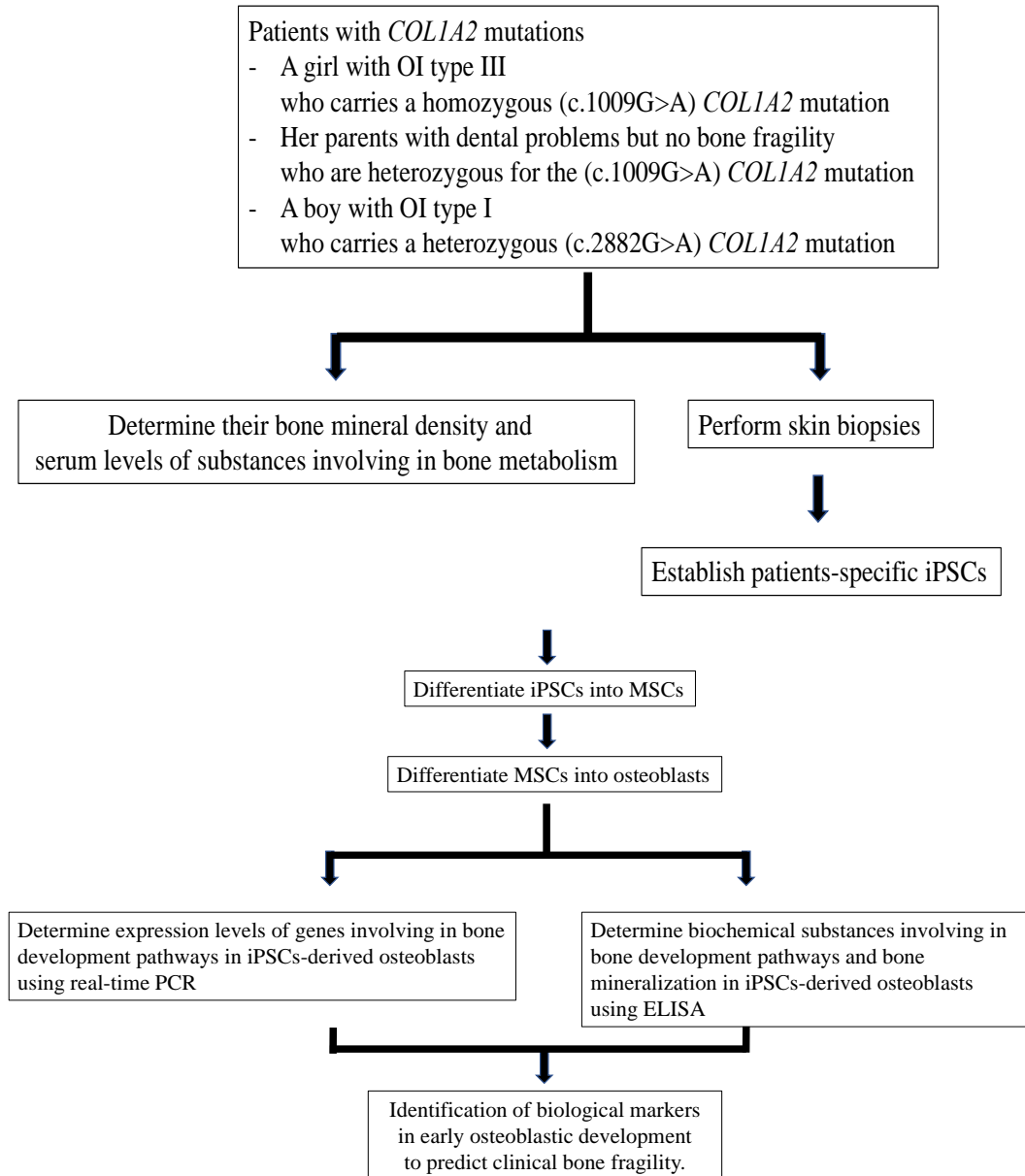
Patient-specific iPSC derived osteoblasts exhibit the deficient osteoblast differentiation and maturation. There is a biochemical substance involving in the human bone development pathway which can serve as a surrogate marker and a cellular phenotype of clinical bone fracture susceptibility in patients with OI.

Objectives

To identify biochemical substances in the OI-patient-specific iPSCs and their differentiated cells, of which levels are different between those with and without clinical OI.

To establish an *in vitro* system to screen for substances which are able to improve OI osteoblasts' functions.

Conceptual framework



Research methodology

1. Participants

The family members with *COL1A2* (c.1009G>A) mutation who parents are consanguineous and carry heterozygous *COL1A2* mutation without a clinical diagnosis of OI but show DI phenotype. Whereas, the daughter with OI type III carries a homozygous *COL1A2* mutation. Besides, a boy with OI type I from an unrelated family who carries heterozygous *COL1A2* (c.2882G>A) mutation was explored in this work. The family's pedigree of OI type patient is shown in Figure 6

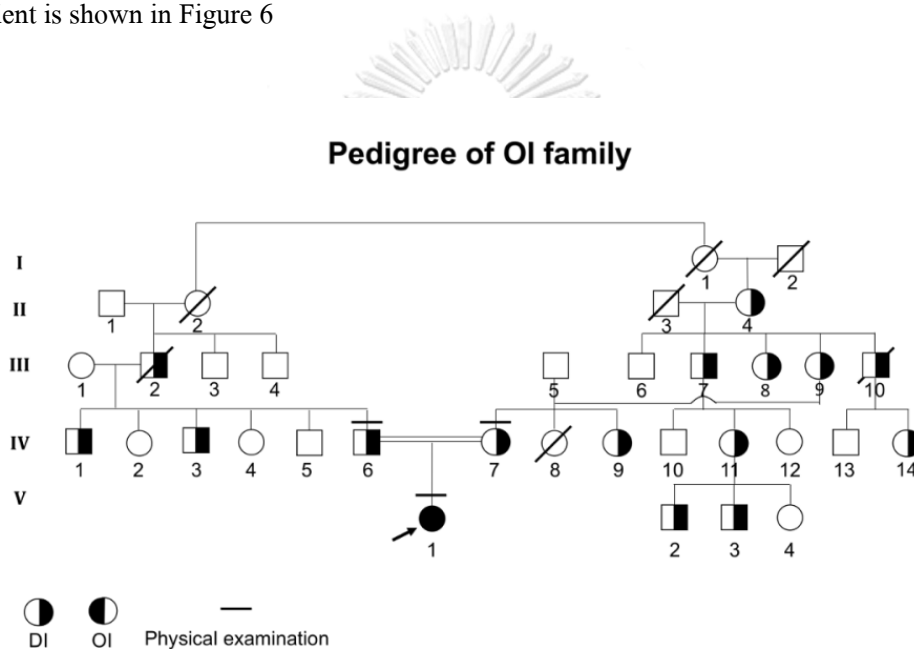


Figure 6 The family's pedigree of proband. The pedigree represents OI is inherited in an autosomal recessive manner while DI is inherited in an autosomal dominant manner in this family.

2. Mutation analysis

Whole exome sequencing (WES) was performed as described (40). Briefly, genomic DNA was isolated from peripheral blood leukocytes using a Puregene Blood kit (QIAGEN). DNA was sent to Macrogen, Inc. (Seoul, South Korea) for WES. DNA was captured using a SureSelect Human All Exon version 4 kit (Agilent Technologies) and sequencing was performed on the a HiSeq2000 instrument. For sequence alignment, variant calling and annotation, sequences were aligned to the human genome reference sequence (UCSC Genome Browser, hg19 build) using BWA aligner (bio-bwa.- sourceforge.net/). Downstream processing was carried out with SAMtools (samtools.sourceforge.net/) and annotated against dbSNP & the 1000 Genomes Project. After quality filtering, the variants were analyzed in 18 OI genes (*FKBP10*, *LEPRE1*, *PIIB*, *BMP1*, *COL1A1*, *COL1A2*, *CREB3L1*, *CRTAP*, *IFITM5*, *MBTPS2*, *PLOD2*, *SERPINF1*, *SERPINH1*, *SP7*, *TMEM38B*, *WNT1*, *SEC24D*, and *SPARC*). All call with coverage <10x; minor allele frequency $\geq 1\%$ in the 1000 Genomes Project and the Exome Aggregation Consortium database (exac.broadinstitute.org); and non-coding variants and synonymous exonic variants were filtered out. The remaining variants were subsequently filtered out if they were present in our in-house database of 1,876 unrelated Thai exomes. The variants in exon 19 of *COL1A2* were validated to be in homozygous state in proband and heterozygous state in parents by PCR and Sanger sequencing. As for pt (FII), sixteen known OI genes (*BMP1*, *COL1A1*, *COL1A2*, *CREB3L1*, *CRTAP*, *FKBP10*, *IFITM5*, *LEPRE1*, *PLOD2*, *PIIB*, *SERPINF1*, *SERPINH1*, *SP7*, *TMEM38B*, *WNT1*, and *MBTPS2*) were amplified from 200 ng of genomic DNA using the Truseq Custom Amplicon Sequencing kit (Illumina, San Diego, CA). The filtering criteria was performed as described above. The variants in exon 44 of *COL1A2* were confirmed in pt (FII) by PCR and Sanger sequencing. Briefly, DNA was amplified by primer as shown in supplementary table 2. The PCR products were treated with Exo-Sap-IT (Affymetrix) followed by Sanger sequencing. RFLP with *MspI* was performed to verify the mutation on genomic DNA of the trio. The digested fragments were separated on a 3% agarose gel. In addition, mutation of *COL1A2* gene of patients iPSCs-derived MSC were analyzed by Sanger sequencing at exon 19 or exon 44. Primers used in PCR amplification and sequencing were shown in Table 2.

3. Generation of patient-specific iPSCs

Skin punch biopsies were obtained from parents while skin biopsies were obtained from OI patients under surgical treatment. Samples were washed several times with 1X PBS. After removal of adipose tissue remnants, samples were dissected into small pieces. Dissected skin pieces were placed on empty the 6 cm² tissue culture dish, and then filled with IMDM (Hyclone)/10% FBS (Hyclone). Once dermal fibroblasts are confluent, they were subsequently subcultured into a new passage and were frozen in completed IMDM media plus 10% DMSO (Invitrogen). Dermal fibroblasts were seeded into 10 cm tissue culture dish and cultured until cells are 80% confluent. iPSCs were generated by using an episomal transfection of Yamanaka factors (OSKM) and Nucleofector for human normal dermal fibroblast kit (Lonza) and Nucleofector™ 2b device (Lonza) following manufacturer instruction manual. Yamanaka factors (OSKM) were provided by Stem cell laboratory, Stem cell and cell therapy research unit, Faculty of Medicine, Chulalongkorn University. Briefly, the dermal fibroblasts of two OI patients were cultured in IMDM supplemented with 10% human umbilical cord serum for three days while the fibroblasts of the proband's parents were maintained in fibroblast medium. The fibroblasts were seeded in the 10-cm plates at the density of 1×10^6 cells per plate overnight. The next day, the culture was dissociated into a single cell, transfected using U-023 program, and seeded in 6-well plates for 24 hours. Then the culture medium was replaced with a mix of fibroblast medium and ES medium (KnockOut DMEM; Invitrogen), 20% (v/v) Knockout Serum Replacement (Invitrogen), non-essential amino acids (NEAA), 1 mM L-glutamine, 0.1 mM β -mercaptoethanol, and 10 ng/ml basic Fibroblast Growth Factor (bFGF; Stemgent). The culture medium was changed to ES medium supplemented with 10 ng/ml bFGF after transfection for 5 days and replaced every day. Within 20-23 days post-transfection, iPSC-liked colonies were manually picked and transferred into human feeder cells and matri-gel coated dishes. Colonies were transferred into mitomycin C (Tocris)-treated human fore skin fibroblast that used as the feeder cells by using the needle. Feeder cells were seeded at 500,000 cells on 0.1% gelatin coated 3.5 mm. dish one day before use. Derived iPSCs were maintained in parallel on feeder cells and in feeder-free condition for at least 2 passage. iPSCs under feeder-free condition were expanded for

further experiments, whereas iPSCs in feeder condition were stored in the liquid nitrogen as the backups. The protocol and timeline of the generation of iPSC were shown in Figure 7. Feeder-free condition refers to the culture dish that coated with the matrigel matrix (Corning) for 1 hour or overnight in 37 °C CO₂ incubator. Human fore skin fibroblast and ESC in the present study were provided by Dr. Ruttachuk Rungsiwiat (41).

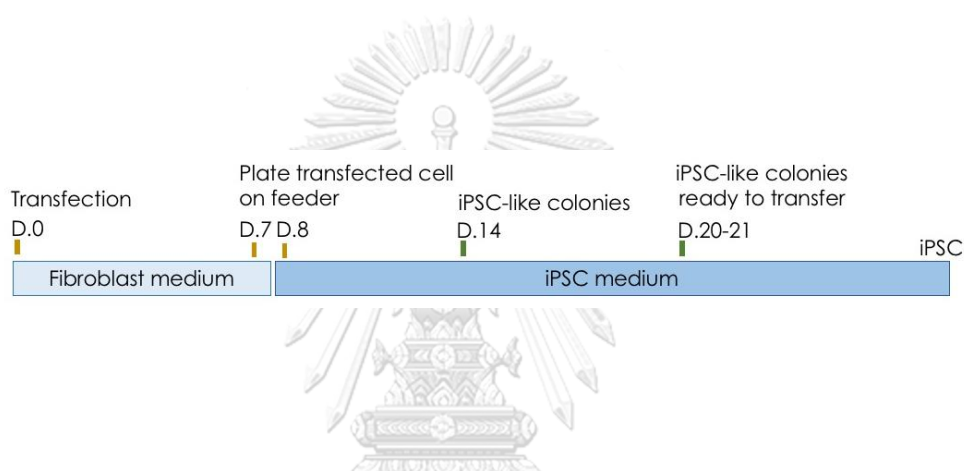


Figure 7 Generation of iPSCs from dermal fibroblast by episomal transfection.

The diagram and timeline for generating iPSCs from dermal fibroblast.

4. Characterization of patient-specific iPSCs

4.1 Expression of pluripotent transcription factor

iPSCs were characterized by expression of pluripotent transcription factor (*NANOG*, *OCT4*, *SOX2*, *REX1*) by RT-PCR and immunofluorescent. iPSCs were cultured and collected to further RNA extraction using RNA blood kit (QIAGEN). RNA was converted into cDNA and was amplified to semi-quantification of a pluripotent gene including *NANOG*, *OCT4*, *SOX2*, and *REX1*. Primers used for RT-PCR were shown in Table 2. The expression of a pluripotent genes was determined by immunofluorescence, which are *TRAI-60*, *TRAI-81*, *NANOG*, and *OCT4*. Briefly, cells were washed with 1XPBS three times and fixed with 4%paraformaldehyde for 15 minutes. After washed three times with 1XPBS, cells that planned to stain for *NANOG* and *OCT4* were permeabilized with 0.1%TRITON X100 for 15 minutes followed by wash with 1XPBS for three times. Cells were treated with PBS containing 1% bovine serum albumin (BSA, VWR) for 30 minutes. After wash with 1XPBS, cells were stained with primary antibody at 4°C overnight. Next, cells were washed with 1XPBS for three times and stained by secondary antibody for 1 hour at room temperature. Finally, cells were counterstained with Hoechst (Life technologies) at 1 ug/ml.

Table 2 Primers for PCR and sequencing

Gene	Primer sequence (5'-3')	Annealing temp.(°c)	Product size (bp)	Ref.
<i>NANOG</i>	F-CAGCCCCGATTCTTCCACCAGTCCC R-CGGAAGATTCCCAGTCGGGTTCCACC	60	391	
<i>OCT4</i>	F-AGCGAACCAGTATCGAGAAC R-TTACAGAACCACACTCGGAC	55	142	(42)
<i>SOX2</i>	F-AGCTACAGCATGATGCAGGA R-GGTCATGGAGTTGTAAGTCA	55	126	(42)
<i>REX1</i>	F-CAGATCCTAACAGCTCGCAGAAT R-GCGTACGCAAATTAAGTCCAGA	58	306	
<i>GAPDH</i>	F-ATCACCATCTTCCAGGAGCGA R-TTCTCCATGGTGGTGAAGACG	58	101	(43)
<i>COL1A2</i> exon19	F-GCA TTT AAT GTG TGC TGC R-GGA AGT CTA GAT AGT GAT GA	58	244	
<i>COL1A2</i> exon 44	F-GGA CAC AAG GTC AGT ACA CT R-CTT ACA GTT TCA CCA CGG	58	208	

Table 3 Primary and secondary antibodies used in immunofluorescence assay

	Markers	Company	Dilution
Pluripotent markers	Mouse anti-TRA1-81	Abcam	1:200
	Mouse anti-TRA1-60	Chemicon (MAB4360)	1:200
	Rabbit anti-NANOG	Cell Signaling Technology (4903)	1:200
	Rabbit anti-OCT4	Cell Signaling Technology (2840)	1:200
	Mouse anti-SSEA-4	Abcam (ab16287)	1:200
Differentiation markers	Mouse anti-NESTIN	Biologend (ab656802)	1:200
	Rabbit anti-BRACHYURY	Abcam (ab20680)	1:200
	Mouse anti-AFP-1	Abcam (ab3969)	1:200
Secondary antibodies	Alexa Fluor 488 Goat anti-Mouse IgG	Life Technologies (A10680)	1:1000
	Alexa Fluor 488 Goat anti-Rabbit IgG	Life Technologies (A11008)	1:1000
	Alexa Fluor 568 Goat anti-Rabbit IgG	Life Technologies (A11036)	1:1000
	FITC anti-mouse IgM	Chemicon (AP500F)	1:500
	Goat anti mouse IgG Cy3	Chemicon (AP181C)	1:500
	Hoechst 33342	Life Technologies (H3570)	1 ug/ml
MSC	PE mouse anti-human CD14	BD Pharmingen™ (562691)	
	APC mouse anti-human CD34	BD Pharmingen™ (555824)	
	PE anti-human CD44	Biologend (338808)	
	PE anti-human CD73	Biologend (344004)	
	Per/CP anti-human CD90	Biologend (328118)	
	APC anti-human CD105	Biologend (323208)	

4.2 *in vitro* differentiation

iPSCs were examined the ability to three lineage differentiation by *in vitro* differentiation. iPSCs were created to form an embryoid body for seven days and were attached to the culture dish. Cells were cultured for twenty-one days and were fixed and analyzed for expression of the three embryonic germline layers markers by immunofluorescence. Endoderm, mesoderm, and ectoderm differentiation were detected by using an antibody against AFP, BRA, and NESTIN, respectively. Primary and secondary antibodies used in immunofluorescence assay were shown in Table 3

4.3 Karyotype analysis

Karyotype of patients iPSCs-derived MSC were performed using G banding standard protocol.

5. Generation of iPSCs-derived MSCs

iPSCs were differentiation to MSC by using either embryoid body (EB) formation or small molecule induction. As for EB formation method, iPSCs were created to form an embryoid body for seven days and were transferred to the gelatin-coated culture dish. Cells were cultured with DMEM high glucose (Hyclone)/10% FBS until the appearance of MSC-like cells. MSC-like cells were dissociated to the new cultured dish at a density of 10,000 cells per cm² into MSC medium, when they confluent. As for small molecule induction, iPSCs were treated with 10 μM SB431542 (Sigma-Aldrich) for 5 days, and then cultured until confluent. Differentiated cells were dissociated to the gelatin-coated dish at a density of 40,000 cells per cm² into MSC medium. Cells were then seeded at 20,000 cells per cm² and at 10,000 cells per cm² with subsequent passages. iPSC-MSC were analyzed for expression of typical MSC markers including CD73, CD105, and CD44. iPSC-MSC will also be determined for lack of broad hematopoietic marker (CD34) and monocyte marker (CD14) expression by flow cytometry. Antibodies used in flow cytometry were shown in Table 2. Briefly, MSCs were dissociated and washed with 1XPBS. MSC at 200,000 cells were incubated with 5 ul of antibody against MSC marker in the dark for 15 minutes. MSCs were subsequently washed with 3 ml of 1XPBS. MSCs were resuspended in 200 ul of 1XPBS.

6. Investigation of the pathways involving osteoblast differentiation

To determine pathways involving bone development, expression of osteogenic markers during osteoblast differentiation were examined. iPSCs-MSC was seeded on a gelatin-coated cultured dish at 10,000 cells per cm². After 3 days, cells were cultured with osteogenic medium containing 0.1 uM dexamethasone (Sigma-Aldrich), 10 mM beta-glycerophosphate (Sigma-Aldrich), and 0.2 mM L-ascorbic acid-2-phosphate (Sigma-Aldrich) which L-ascorbic acid-2-phosphate was only added first 2 times of the medium replacement. Medium was changed every other day up to 3 weeks. As for the conditioned medium collection, the medium was changed day 4, 6, 11, and 19. Cell lysate and conditioned medium was collected at day 5, 7, 12, and 20 with TRIZOL reagent (Invitrogen) and RIPA buffer (Thermo Fisher Scientific) for RNA extraction and protein analysis, respectively. Osteoblasts were collected using TRIZOL (Invitrogen) for mRNA isolation. cDNA was synthesized using ImProm-II (Promega) by using 500 ng of RNA as the template in the total volume 20 ul of the reaction. Gene expression quantification was performed by qPCR (StepOnePlus: Applied Biosystems) using TaqMan probe (Applied Biosystems). The expression level of *COL1A1*, *COL1A2*, *ALP*, *OC*, *SPP1* (OPN) was normalized to the level of *GAPDH*. Probes for real-time PCR were shown in table 4. Briefly, qPCR reaction composed of 1 ul of cDNA, 10 ul of Luna universal qPCR master mix (NEB), 1 ul of probe, and 8 ul of nuclease free water. As for *OC*, the qPCR reaction composed of 5 ul of cDNA. The experiments were performed in triplicate. Data were analyzed by SPSS software. For group comparisons, the significant differences were determined using either one-way ANOVA followed by Turkey Post post hoc test or independent sample t-test as appropriate. Statistical significance was considered at p-value < 0.05.

7. Type I collagen detection

Type I collagen from cultured medium was isolated according to the previous reports (44). Condition medium was collected and buffered with 100 mM Tris-HCl, pH 7.4, and cooled

to 4°C overnight. Protease inhibitors were added to the following final concentrations: 25 mM EDTA, 0.02% NaN₃, 1 mM phenylmethylsulfonylfluoride, 5 mM benzamidine, and 10 mM N-ethylmaleimide. Procollagens were precipitated from medium with ammonium sulfate overnight at 4°C. Procollagen was collected by centrifugation at 12,000 x g for 60 minutes at 4°C, resuspended in 0.5 M acetic acid and digested with 0.1 mg/ml pepsin at 4°C overnight. Selective salt precipitation of collagen with 0.9 M NaCl in 0.5 M acetic acid was performed twice. Purified collagen samples were resuspended in 0.1 M acetic acid and was analyzed on 8% SDS urea-PAGE gels. Protein and prestained protein ladder (Abcam, ab116029) were run under the non-reducing condition in 8% SDS urea-PAGE gels on ice for 5-6 hours and then stained by Bio-safe coomassie stain (BIO-RAD) followed the manufacturer protocol.

8. Investigation of biochemical substances involving mineralization

To study biochemical substances which is osteogenic marker responsible for the bone development, level of osteogenic markers expressed in the culture medium were explored. Osteocalcin and osteopontin secreted into culture medium were performed by commercial ELISA kit (R&D Systems) follow the instruction manual. Type I collagen synthesis was analyzed by using procollagen type I C-propeptide (PIP, TAKARA) follow the instruction manual. The experiments were performed in duplicate. Data were analyzed by SPSS software. For group comparisons, the significant differences were determined using independent sample t-test as appropriate. Statistical significance was considered at p-value < 0.05. Total protein was analyzed by BCA protein assay (Pierce).

Alizarin R staining was performed to determine the calcium deposit of osteoblast. Briefly, after wash three time with 1XPBS, osteoblasts were fixed with 4%paraformaldehyde for 15 minutes at room temperature. Cells were washed three times with sterile distilled water and incubated for 45 minutes with 40 mM alizarin red (Sigma-Aldrich) in distilled water and adjust pH to 4.1-4.3. Alizarin solution was carefully aspirated and cells were carefully washed with distilled water for three times and left to dry.

Table 4 Probes for real-time PCR

Gene	Taqman gene expression assay
Alkaline phosphatase (<i>ALP</i>)	Hs1029144_m1
Bone gamma-carboxyglutamate protein/Osteocalcin (<i>BGLAP/OC</i>)	Hs01587814_g1
Collagen type I alpha 1 (<i>COL1A1</i>)	Hs00164004_m1
Collagen type I alpha 1 (<i>COL1A2</i>)	Hs01028969_m1
Glyceraldehyde-3-phosphate dehydrogenase (<i>GAPDH</i>)	Hs02758991_g1
Secreted Phosphoprotein 1/Osteopontin (<i>SPP1/OPN</i>)	Hs00959010_m1

Administration and time schedule

Table 1 Administration and time schedule

	Month									
	1-4	5-8	9-12	13-16	17-20	21-24	25-28	29-32	33-36	
Review of related literatures		←————→								
Prepare primary fibroblast cell culture of participants		↔								
Generate patients-specific iPSCs		←————→								
Characterize iPSCs			←————→							
Generate MSC derived from iPSC and characterize iPSCs derived MSC				←————→						
Investigate type I collagen synthesis						←————→				
Investigate expression of osteogenic markers during osteoblast differentiation							←————→			
Investigate level of biochemical substance involving bone formation during osteoblast differentiation								←————→		

Results

1. Clinical data

Proband is Thai girl who was born in the consanguineous family in 2002. She was referred to Center of Excellence for Medical Genomics, Department of Pediatrics, Faculty of Medicine, Chulalongkorn University at age 13 years. She received evaluation including medical history, physical examination, and X-ray film. The family's pedigree of proband is shown in Figure 6. As shown in Figure 8A-N, radiograph show short stature, triangular face, barrel chest and severe bone deformity, scoliosis, curved, slender bones, multiple fractures and intramedullary rods were used to stabilize the fractures. She had blue sclerae and dentinogenesis imperfecta (DI). Her parents show normal bone, lack signs and symptoms of skeletal fragility, while show DI phenotype (Figure 9). Bone mineral density of lumbar spine of proband was 0.404 g/cm^2 (z-score -5.6). The lumbar spine BMD of the father at age 43 years was 0.724 g/cm^2 (z-score -1.7) and of the mother at age 37 years was 0.972 g/cm^2 (z-score -0.2).

Gene alteration of proband was analyzed by whole exome sequencing which revealed the homozygous c.1009G>A (p.G337S) mutation in *COL1A2* gene (Table 6). Then, her parents were indentified for *COL1A2* mutation that show heterozygous c.1009G>A (p.G337S) *COL1A2* mutation. Besides, a boy with OI type I from an unrelated family who carries heterozygous *COL1A2* (c.2882G>A, p.G961D) mutation were also explored by targeted gene sequencing panel (Table 7).

Mutation analysis of trio and pt (FII) have been confirmed by Sanger sequencing (Figure 10A) which done by Mr.Chalurmpon Srichomthong. The homozygous c.1009G>A (p.G337S) mutation in *COL1A2* gene was confirmed by RFLP analysis (Figure 10B).

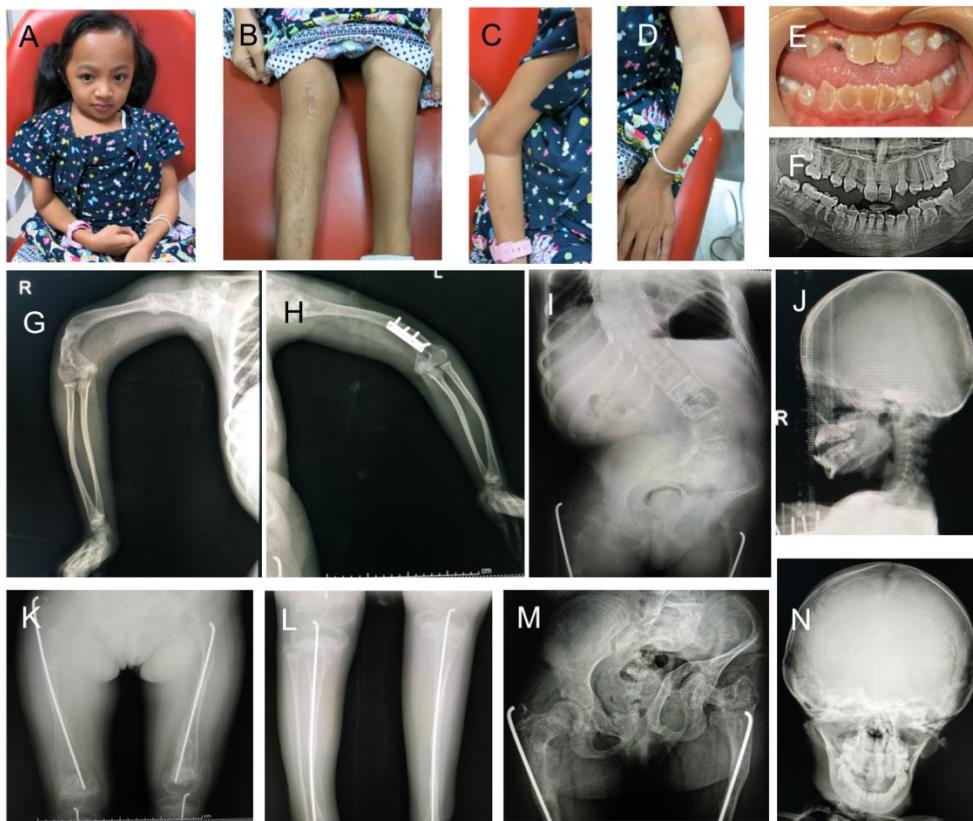


Figure 8 Clinical features associated with proband. The photographs and radiographs display the clinical phenotype of proband.

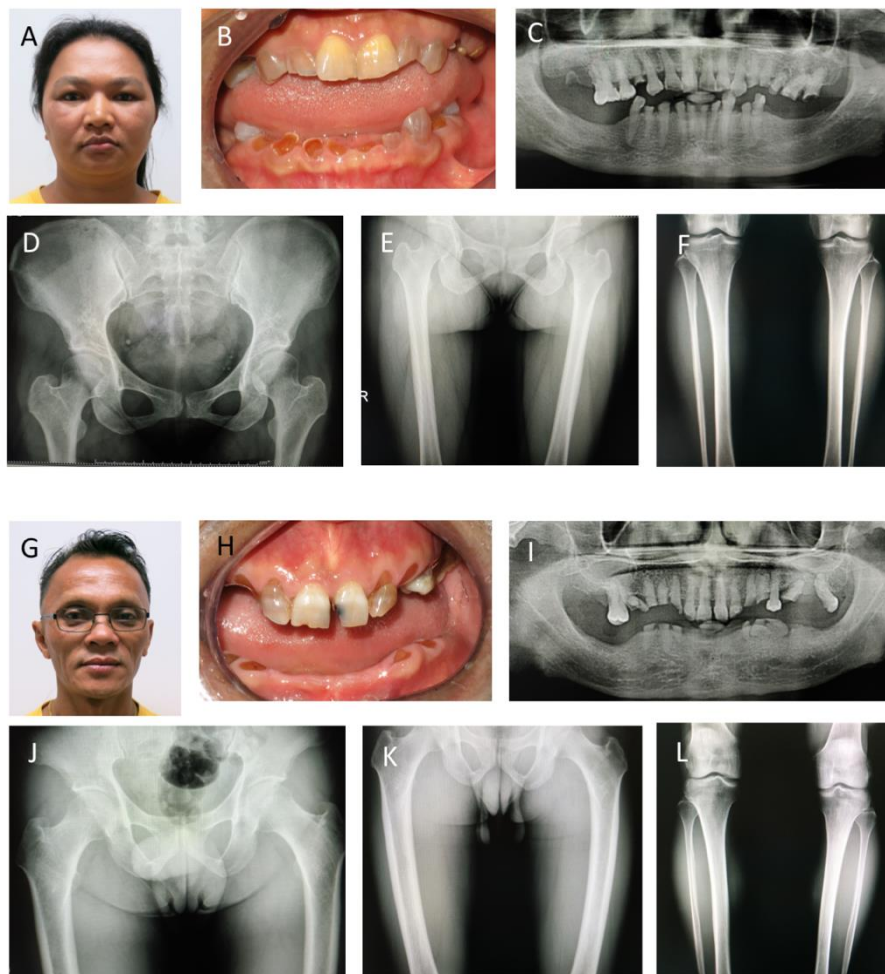


Figure 9 Clinical features associated with mother and father of proband. The photographs and radiographs display the clinical phenotype of mother (A-F) and father (G-L).

Table 5 Filtering criteria for the exome sequencing of proband

Filtering criteria	Result
Total number of variants after variants calling (1000 Genomes Project Consortium, dbSNPs)	15357 genes/ 78491 variants
After filtering with 18 OI genes (<i>FKBP10, LEPRE1, PPIB, BMP1, COL1A1, COL1A2, CREB3L1, CRTAP, IFITM5, MBTPS2, PLOD2, SERPINF1, SERPINH1, SP7, TMEM38B, WNT1, SEC24D, and SPARC</i>)	14 genes/ 89 variants
After filtering for pathogenic mutation	8 genes/11 variants
After variant annotation and filtering with exclusion of variants with coverage <10x; minor allele frequency > 1% in the 1000 Genomes Project and EXAC; and non-coding variants and synonymous exonic variants	3 genes/4 variants
After exclusion of variants found in an in-house database of 1,876 Thai exomes	1 genes/1 variants
Gene	<i>COL1A2</i>
Variant	G>A
Coordinate	7: 94039107
Genotype	Homozygous
Transcript	NM_000089.3
Consequence	missense variant
cDNA	c.1009G>A
Protein	p.(Gly337Ser)
Sift	deleterious (0)
PolyPhen-2	probably damaging (1)
M-CAP	Possibly pathogenic (0.856)

Table 6 Filtering criteria for the exome sequencing of pt (FII)

Filtering criteria	Result
After filtering with 16 OI genes (<i>BMP1</i> , <i>COL1A1</i> , <i>COL1A2</i> , <i>CREB3L1</i> , <i>CRTAP</i> , <i>FKBP10</i> , <i>IFITM5</i> , <i>LEPRE1</i> , <i>PLOD2</i> , <i>PPIB</i> , <i>SERPINF1</i> , <i>SERPINH1</i> , <i>SP7</i> , <i>TMEM38B</i> , <i>WNT1</i> , and <i>MBTPS2</i>)	16 genes/ 145 variants
After filtering with variant QC	16 genes/ 110 variants
After filtering for pathogenic mutation	6 genes/10 variants
After variant annotation and filtering with exclusion of variants with coverage <10x; minor allele frequency > 1% in the 1000 Genomes Project and EXAC; and non-coding variants and synonymous exonic variants	3 genes/5 variants
After exclusion of variants found in an in-house database of 1,876 Thai exomes	1 gene/1 variants
Gene	<i>COL1A2</i>
Variant	G>A
Coordinate	7:94055108
Genotype	Heterozygous
Transcript	NM_000089.3
Consequence	missense variant
cDNA	c.2882G>A
Protein	p.(Gly961Asp)
Sift	deleterious (0)
PolyPhen-2	probably damaging (1)
M-CAP	Possibly pathogenic (0.913)

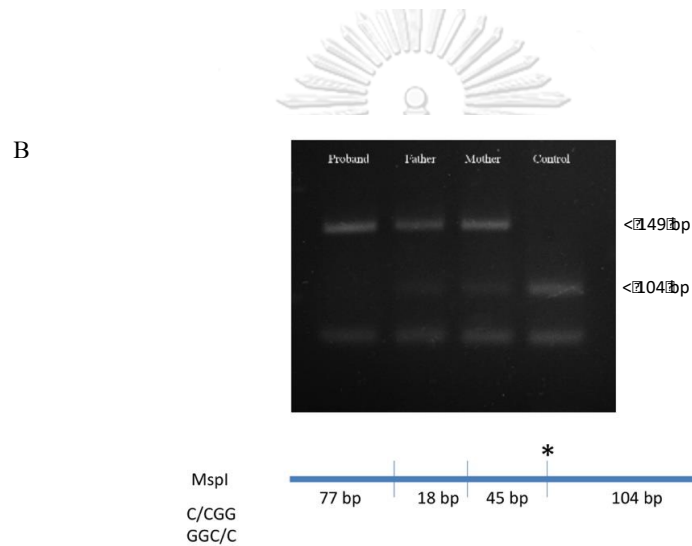
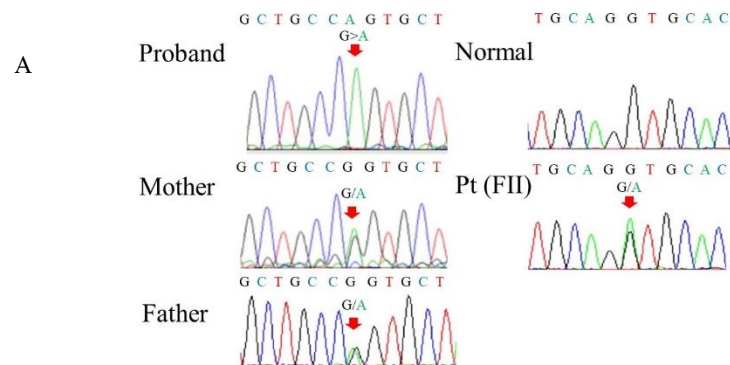


Figure 10 Mutation analysis of trio. (A) Chromatograms show mutation in *COL1A2* exon 19 of the trio, and *COL1A2* exon 44 of pt (FII). (B) RFLP shows only mutant band of 149 bp in proband while father and mother show both mutant band and wildtype band of 104 bp.

2. Generation of patients-specific iPSCs

Patient-specific iPSC generated from dermal fibroblast of the father, mother, and daughter with OI type III are called iPSC father, iPSC mother, and iPSC proband respectively. Patient-specific iPSC generated from dermal fibroblast of a boy with OI type I is called iPSC pt (FII). The number of an established patient-specific iPSC cell line from all participants were displayed in Table 8. Figure 11A shows iPSC-like colony after 20 days of the transfection. Figure 11B shows iPSC-like colony on day 6 after transferring into matrigel. Figure 11C exhibits the established iPSC of proband which is cultured in feeder-free condition and displays the cell morphology like iPSC. iPSCs exhibit round morphology with well-defined sharp edges and contain tightly packed cells. Individual cells within the colony exhibit prominent nucleoli with a high ratio of nucleus to cytoplasm volume ratio.

Table 7 Number of established patient-specific iPSC cell line from all participants

Patients-specific iPSCs	iPSC clone numbers
Pt (FII) iPSC	4
Proband iPSC	8
Father iPSC	11
Mother iPSC	12

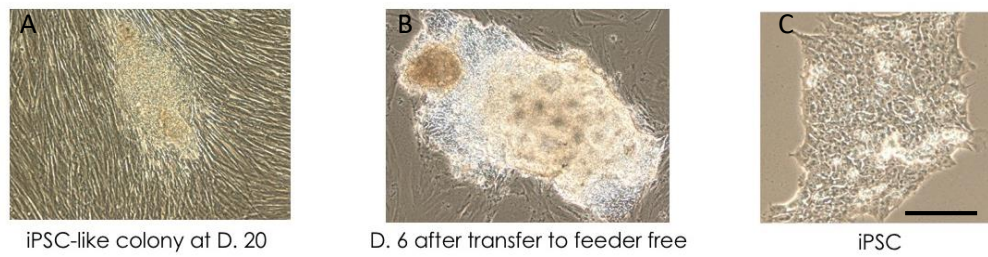


Figure 11 The established iPSC of proband. Photographs exhibit iPSC-like colony on day 20 after transfection (A), iPSC-like colony on day 6 after transferring into matrigel (B), and morphology of proband iPSC on matrigel (C). Scale bar = 400 μm



3. Characterization of patient-specific iPSCs

3.1 Expression of pluripotent transcription factors

RT-PCR analysis showed that the established patient-specific iPSC cell line (father, mother, proband, pt (FII)) expressed endogenous pluripotent genes including *OCT4*, *SOX2*, *REX1* and *NANOG* (Figure 12).

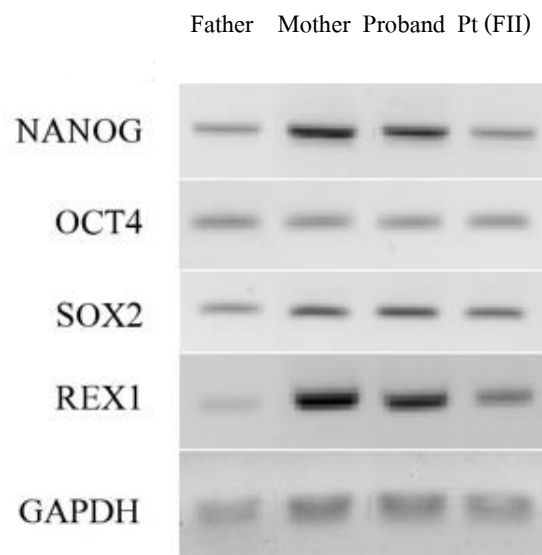


Figure 12 Expression of pluripotent transcription factors. PCR analysis of pluripotent markers of patient-specific iPSCs. GAPDH was used as the loading control.

3.2 Immunocytochemical staining

Immunocytochemical staining exhibited positive results with pluripotent markers TRA1-1-60, TRA1-81, NANOG, and OCT4 in all of established patient-specific iPSC cell lines (father, mother, proband, pt (FII)) (Figure 13). TRA1-60 and TRA1-81 were displayed surface staining, whereas NANOG and OCT4 was showed intracellular staining. Hoechst 33342 stained the nuclei as blue color.

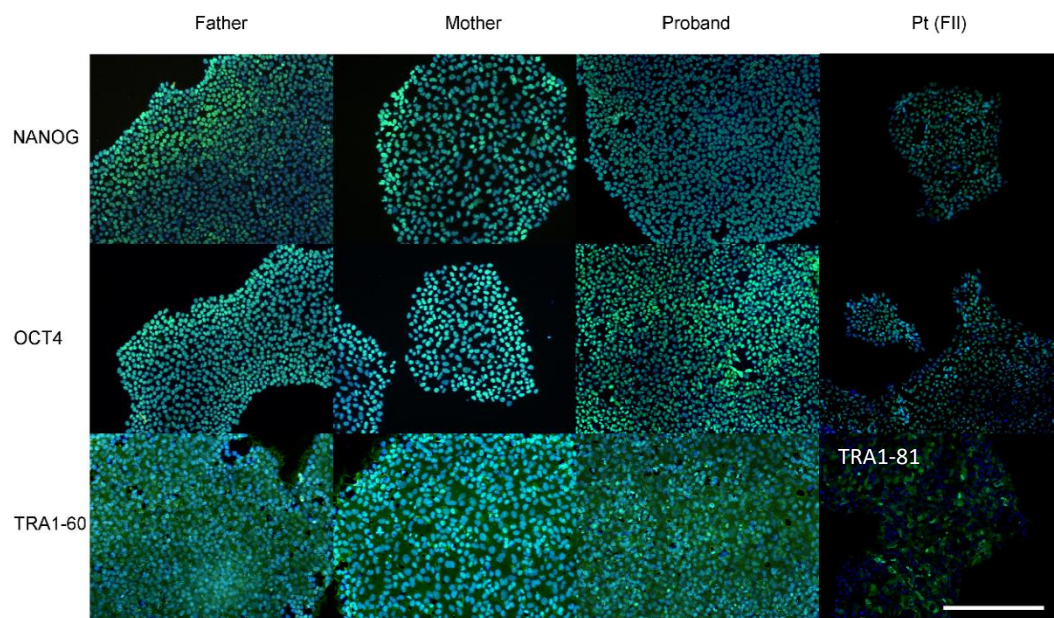


Figure 13 Immunocytochemical staining of pluripotent markers. NANOG, OCT4, TRA1-60, and TRA1-81 represent in green color. Scale bar = 400 μm

3.3 *in vitro* differentiation

All of iPSC lines were cultured in EB suspension for 7 days followed by additional cultured for 14 days in matri-gel coated plate to promote the *in vitro* differentiation towards the three germ layer derivatives. After EBs were cultured for 14 days, differentiated cells exhibited the positive result of immunoreactive for ectodermal (NESTIN, NES), mesodermal (BRACHYURY, BRA) and endodermal (AFP) marker (Figure 14).

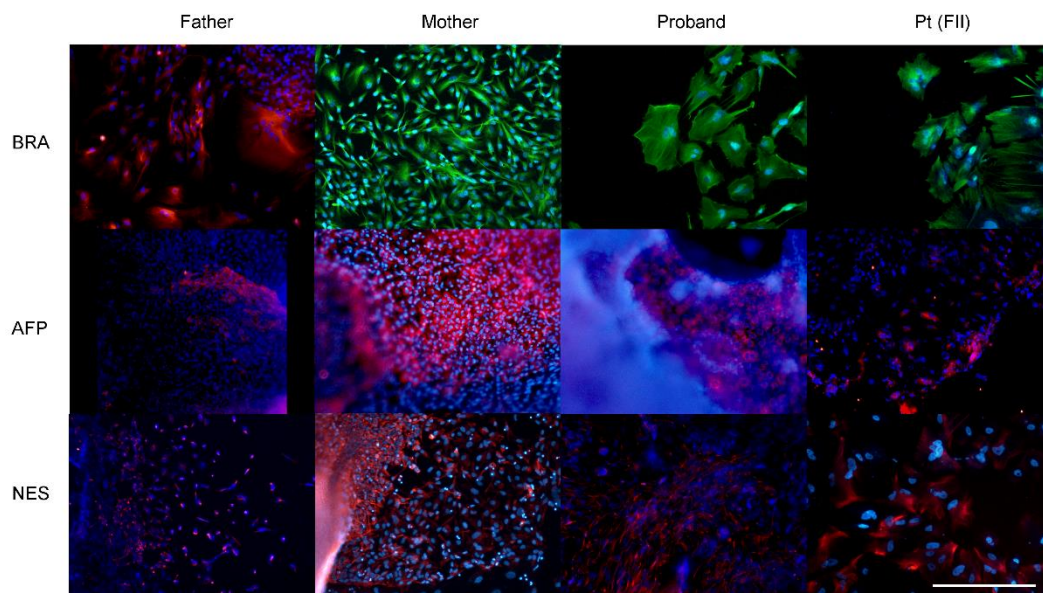


Figure 14 Immunocytochemical staining of three-germ layer markers. BRA in father displays in red color while that of in mother, proband, and pt (FII) present in green color. AFP and NES of trio and pt (FII) show in red color. Scale bar = 400 μm

3.4 Mutation analysis

Mutation in *COL1A2* gene of established patient-specific iPSC-derived MSCs was confirmed by Sanger sequencing. As for trio, the mutation was analyzed using specific primer for *COL1A2* exon 19, while pt (FII) was analyzed using specific primer for *COL1A2* on 44. Figure 14 showed G to A substitution at nucleotide position 1009 of *COL1A2* gene, which is the heterozygous mutation of father, mother, and homozygous *COL1A2* mutation of proband, respectively. Figure 15 showed the heterozygous *COL1A2* mutation in exon 44 of pt (FII), which is G to A substitution at nucleotide position 2882.

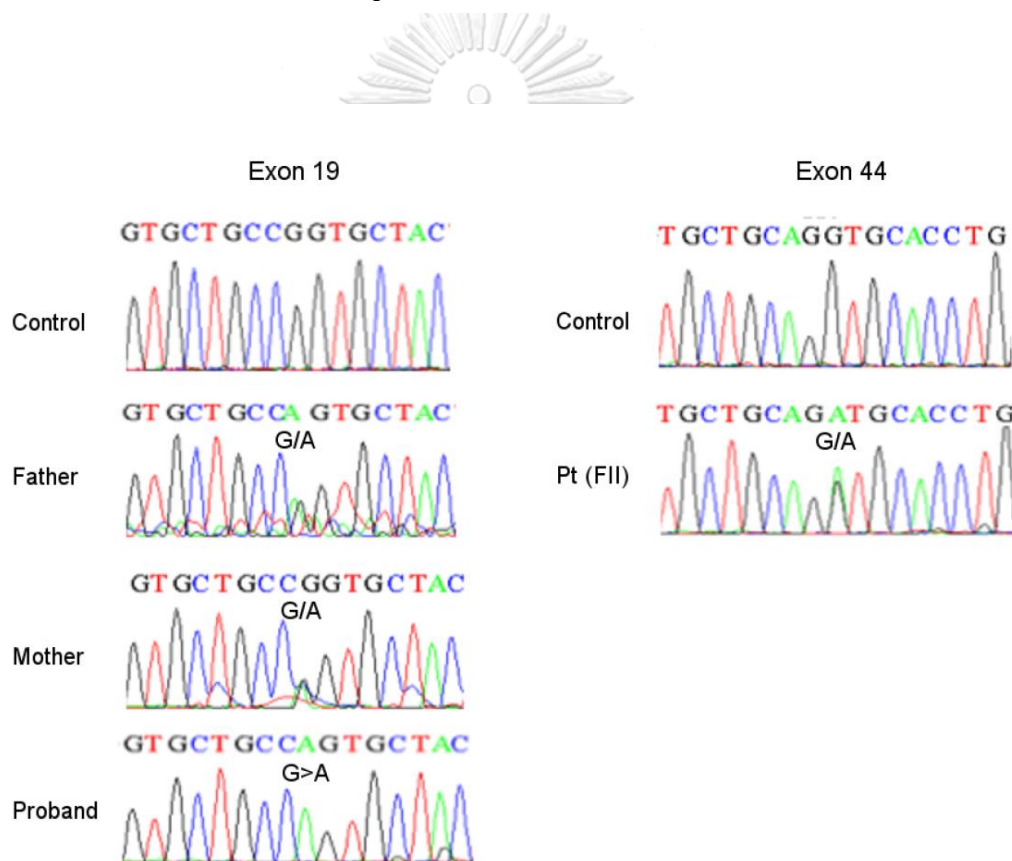


Figure 15 Electrochromatogram of the mutation in exon 19 and 44 of *COL1A2* gene. Sanger sequencing shows G to A substitution in exon 19 and exon 44 of *COL1A2* gene in trio and pt (FII), respectively.

4. Generation of iPSCs-derived MSCs

Father, mother and proband iPSC were differentiated to MSC by using EB formation. Control ES was differentiated to MSC by using spontaneous differentiation protocol. Whereas, pt (FII) was differentiated to MSC by using small molecule induction by treat with SB431542 at 10uM according to previous report (45). After iPSC-derived MSC and ES-derived MSC were passage as the homogenous population, they were analyzed the expression of MSC markers by flow cytometry. Figure 16 shows iPSC-derived MSCs that exhibit spindle-like morphology.

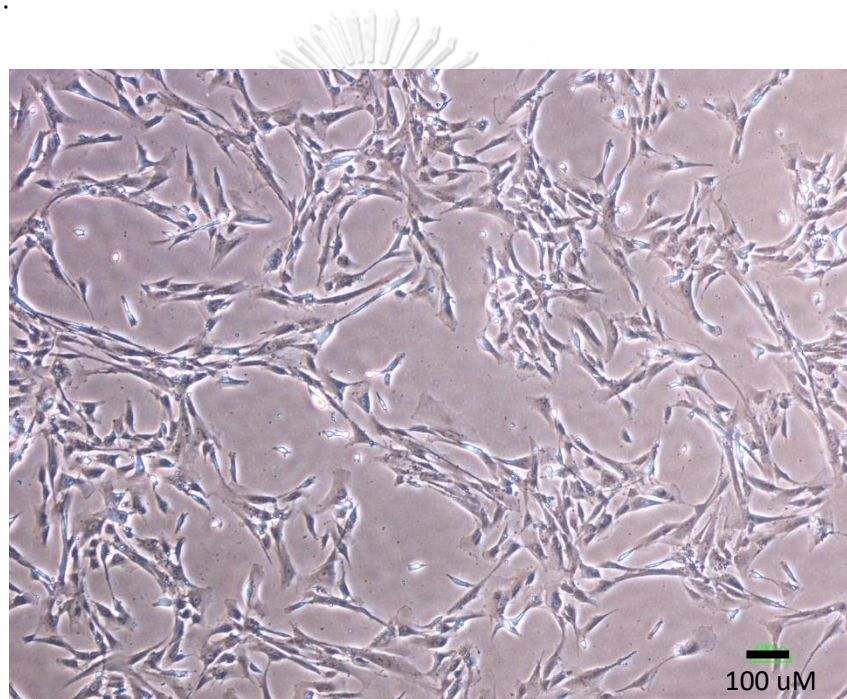


Figure 16 Morphology of proband iPSC-derived MSC. Cells display long and spindle-like morphology. Scale bar = 100 μm

5. Flow cytometry analysis

Control ESC and established patient-specific iPSC were efficiently differentiated to MSC as mention above. They were determined for expression of MSC markers, which are CD44, CD73, and CD105, and also determined for lack of expression of the hematopoietic marker CD14 and CD34.

Table 8 Level of surface marker expressed on iPSCs-derived MSCs

	CD44	CD73	CD105	CD14	CD34
Father-MSC	98.5	100	99.8	0	0
Mother-MSC	100	99.9	99.6	0	0
Proband-MSC	99.9	99.7	97.1	0	0
Pt (FII)-MSC	99.7	99	72.4	0	0
ES-MSC	99.9	100	99.6	0	0

6. Karyotype analysis

Karyotype analysis was performed in either established patient-specific iPSC or iPSC-derived MSC. Father-derived MSC (Figure 17A) and pt (FII) (Figure 17D) displayed a normal diploid 46, XY karyotype. As for mother-derived MSC (Figure 17B) and proband-derived MSC (Figure 17C), chromosome analysis showed a normal diploid 46, XX karyotype. All of iPSC-derived MSC have no appreciable abnormalities of karyotype.

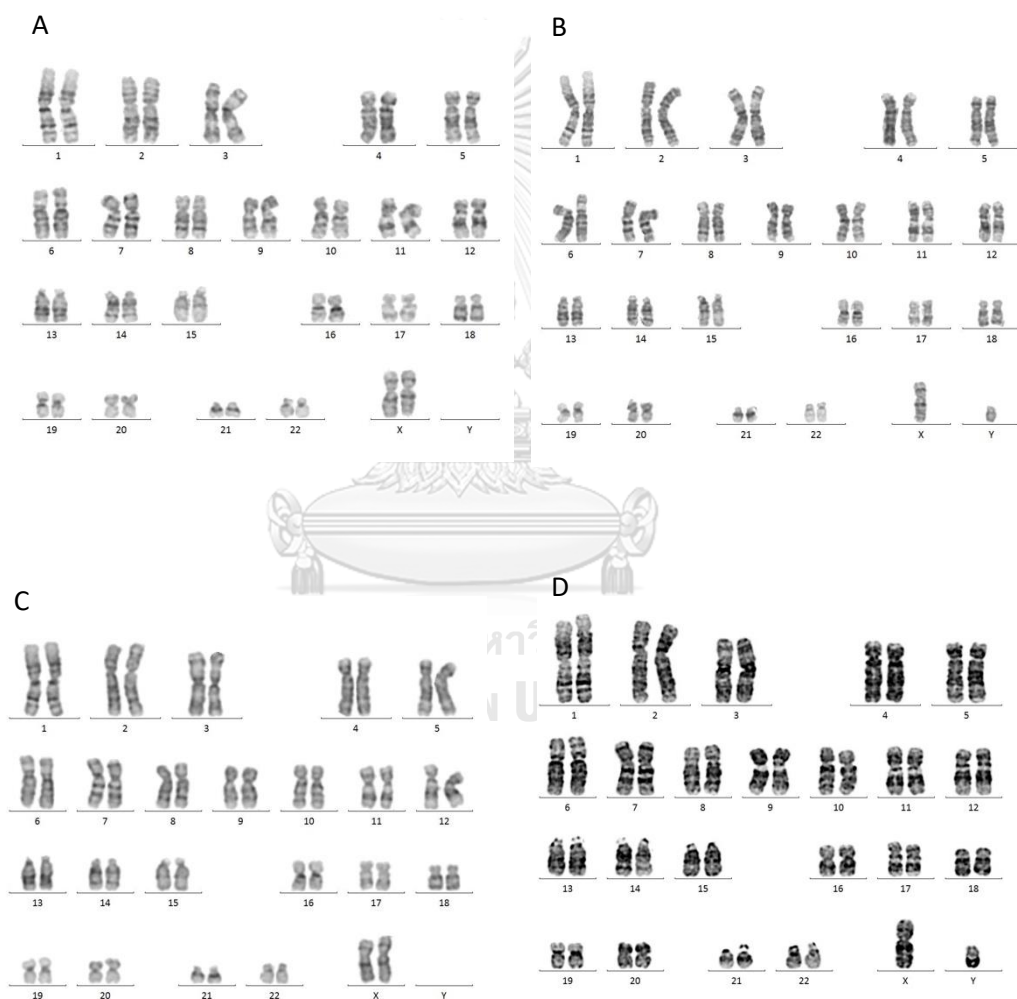


Figure 17 Karyotype analysis of iPSCs-derived MSCs. Karyotype analysis of iPSCs using G banding showed normal karyotypes. A, B, C, and D represent karyotype of father, mother, proband, and pt (FII), respectively.

7. Investigation of type I collagen synthesis and overmodification

7.1 Type I collagen detection

Secreted collagen I of each sample were run in SDS-urea PAGE. Collagen I was migrated and separated into 2 band according to $\alpha 1(I)$ and $\alpha 2(I)$ chain. $\alpha 1(I)$ chain of collagen I obtained from pt (FII) displayed shift band due to the overmodification while trio had no detectable abnormality (Figure 18).

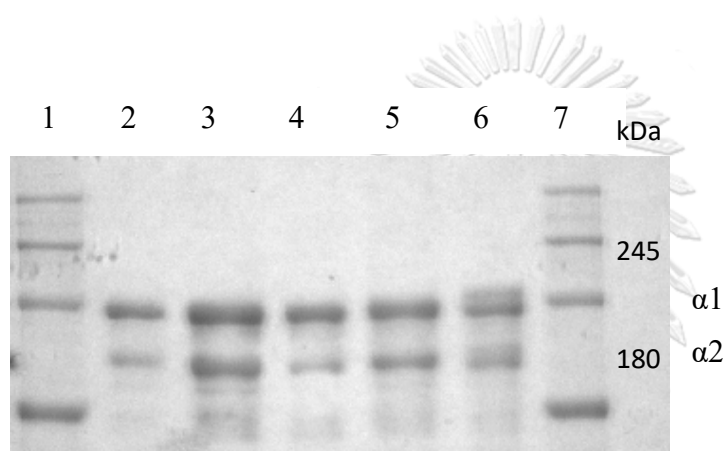


Figure 18 Collagen I secreted from MSCs-derived osteoblasts. Upper and lower band represent $\alpha 1$ and $\alpha 2$ chain of collagen I produced by ESC-derived MSC (2), father iPSC-derived MSC (3), mother iPSC-derived MSC (4), proband iPSC-derived MSC (5) and pt (FII) iPSC-derived MSC (6). Lane 1 and 7 are prestained protein ladder.

7.2 Type I collagen synthesis

Type I collagen synthesis in the culture medium during osteoblast differentiation of each iPSC derived osteoblast was determined by PIP ELISA assay at day 0, 5, 7, and 12 after treated with osteogenic induction medium. The ES-derived MSC was used as the control. Level of PIP (ng) was normalized per total protein (mg). The result shows that the level of PIP in all of patient iPSC-derived MSCs was lower than that of the control (Figure 19).

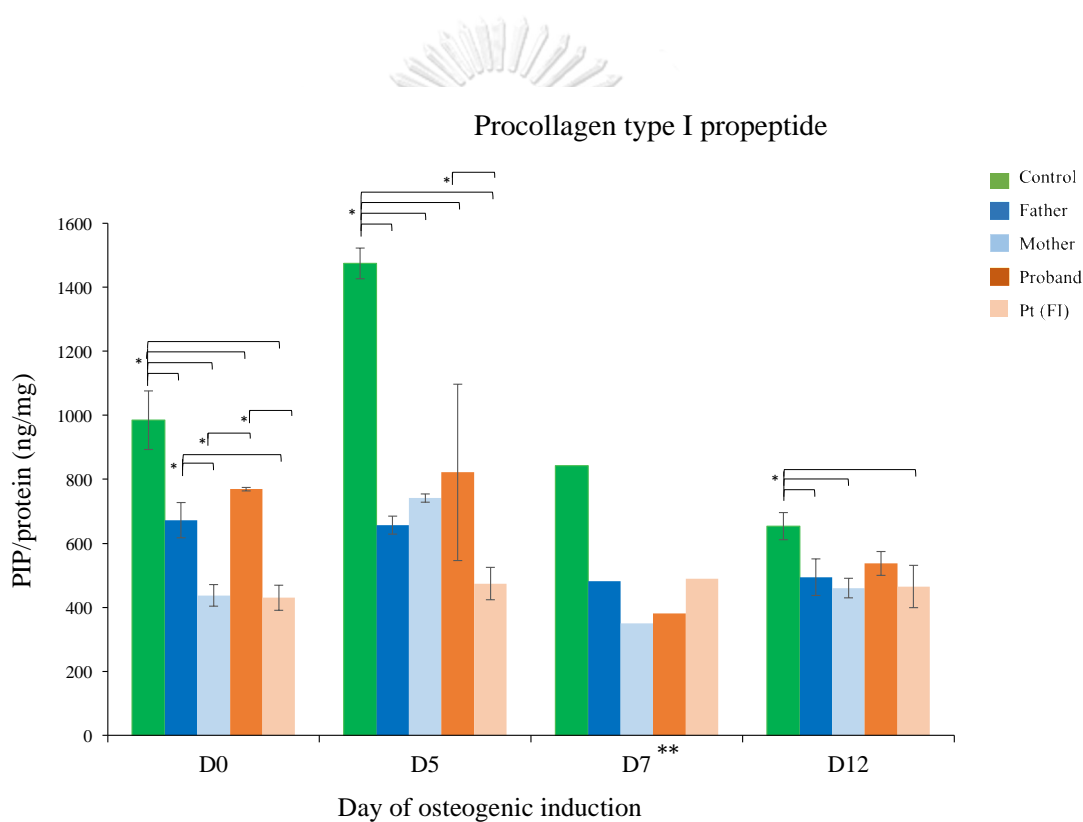


Figure 19 Level of procollagen I propeptide (PIP). PIP represents type I collagen synthesis in the control, and patients without OI and with OI. *p<0.05, **N=1

8. Investigation of osteogenic gene expression involving osteoblast differentiation

8.1 Real-time PCR

All iPSC-derived MSC and ESC-derived MSC were differentiated into osteoblast, and then the expression of osteogenic markers (*COL1A1*, *COL1A2*, *SPP1* (OPN), *OC*, and *ALP*) were determined by real-time PCR. The expression level of iPSC-derived MSC were compared with ESC-derived MSC at different time point, which were day 5, 7, and 12. The result shows that the expression of *COL1A1* was significant differences among all patient iPSC-derived osteoblast at day 5 and both of OI iPSC-derived osteoblast was significantly downregulated when compared with father and mother iPSC-derived osteoblast patient at day 12 (Figure 20). Expression of *COL1A2* was a statistically significant difference in all iPSC-derived osteoblast at day 5 and day 7 and both of OI iPSC-derived osteoblast was significantly low expressed compared to father and mother iPSC-derived osteoblast at day 12 (Figure 21). Expression of *SPP1* (OPN) was detected in ESC-derived MSC and father iPSC-derived MSC, whereas it was low expressed in mother and proband iPSC-derived MSC and it was not detected in pt (FII) iPSC-derived MSC. *SPP1* was markedly peak in ESC-derived MSC at the early time course and reduce at day 12 (Figure 22). Expression of *OC* in proband and pt (FII) iPSC-derived MSC showed significantly downregulated when compared with ESC and mother iPSC-derived MSC at day 5 (Figure 23). Expression level of *ALP* was statistically significant difference in control when compared with trio and pt (FII) at day 5. *ALP* was equally high in trio iPSC-derived MSC in day 5. *ALP* expression level in proband iPSC-derived MSC was lower than father and mother iPSC-derived MSC in day 12. Interestingly, *ALP* was not detected in pt (FII) iPSC-derived MSC along the time course of osteoblast differentiation. (Figure 24)

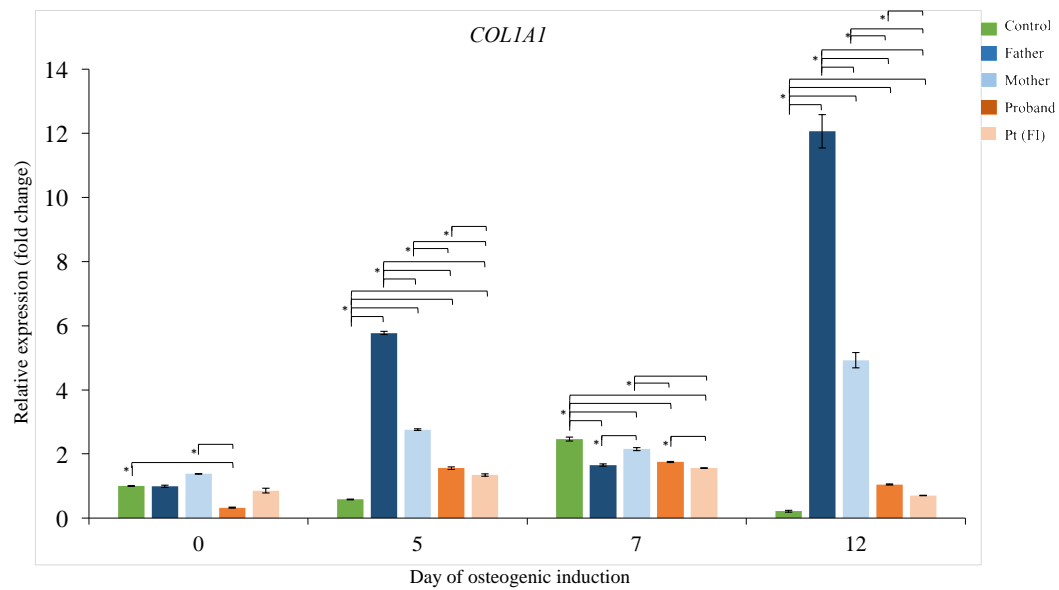


Figure 20 Expression of *COL1A1* gene. Level of *COL1A1* expression in ESC and patient iPSC-derived MSC during osteoblast differentiation at day 0, 5, 7, and 12 which was assayed by real-time PCR and represented as the relative expression in the fold of the control. The ESC-derived MSC was used as the control. * $p < 0.05$ compared to each other.

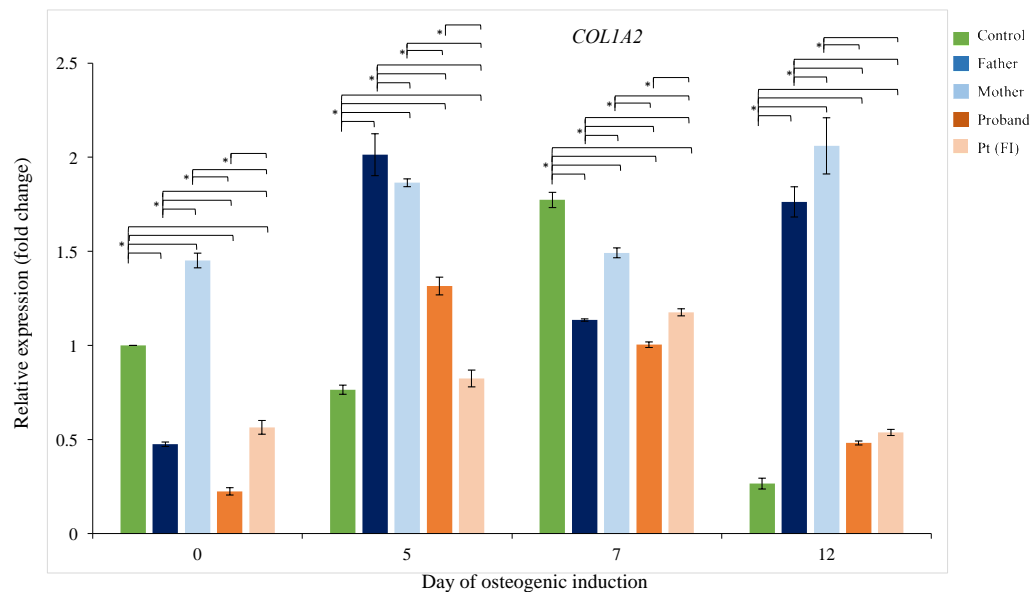


Figure 21 Expression of *COL1A2* gene. Level of *COL1A2* expression in in ESC and patient iPSC-derived MSC during osteoblast differentiation at day 0, 5, 7, and 12 which was assayed by real-time PCR and exhibited as the relative expression in the fold of the control. The ESC-derived MSC was used as the control. * $p < 0.05$ compared to each other.

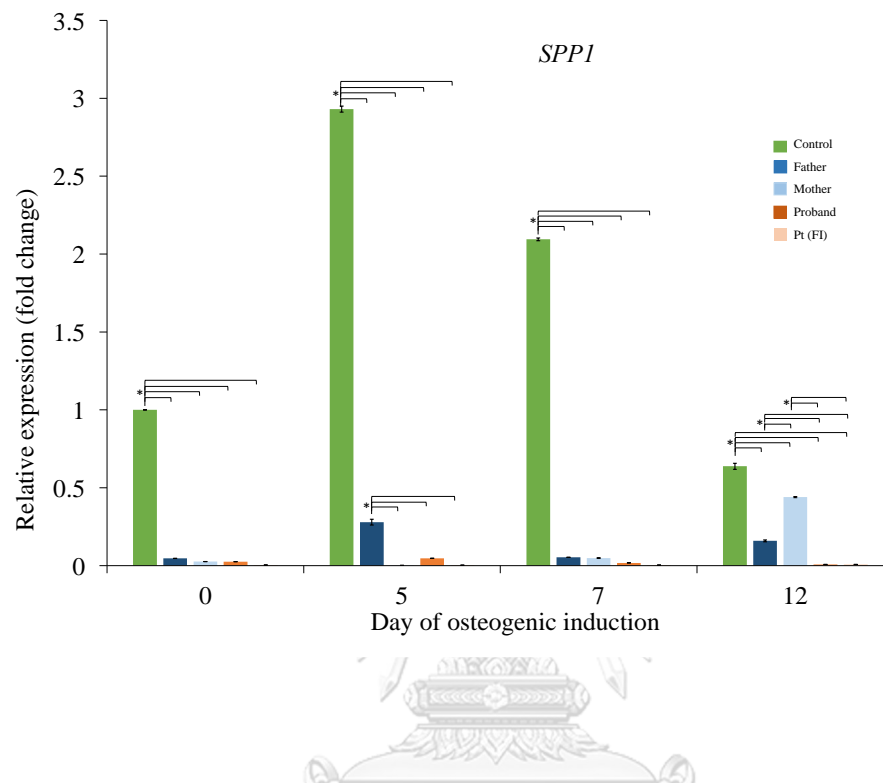


Figure 22 Expression of *SPP1* (OPN) gene. Level of *SPP1* expression in in ESC and patient iPSC-derived MSC during osteoblast differentiation at day 0, 5, 7, and 12 which was assayed by real-time PCR and showed as the relative expression in the fold of the control. The ESC-derived MSC was used as the control. * $p < 0.05$ compared to each other.

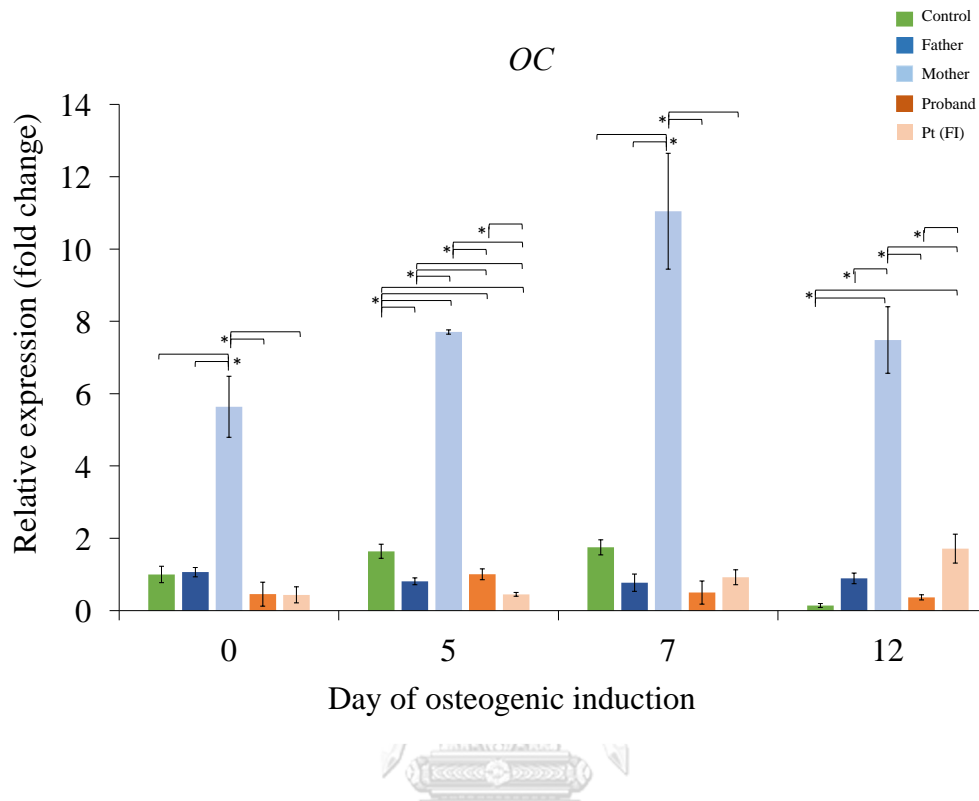


Figure 23 Expression of *OC* gene. Level of *OC* expression in in ESC and patient iPSC-derived MSC during osteoblast differentiation at day 0, 5, 7, and 12 which was assayed by real-time PCR and expressed as the relative expression in the fold of the control. The ESC-derived MSC was used as the control. * $p < 0.05$ compared to each other.

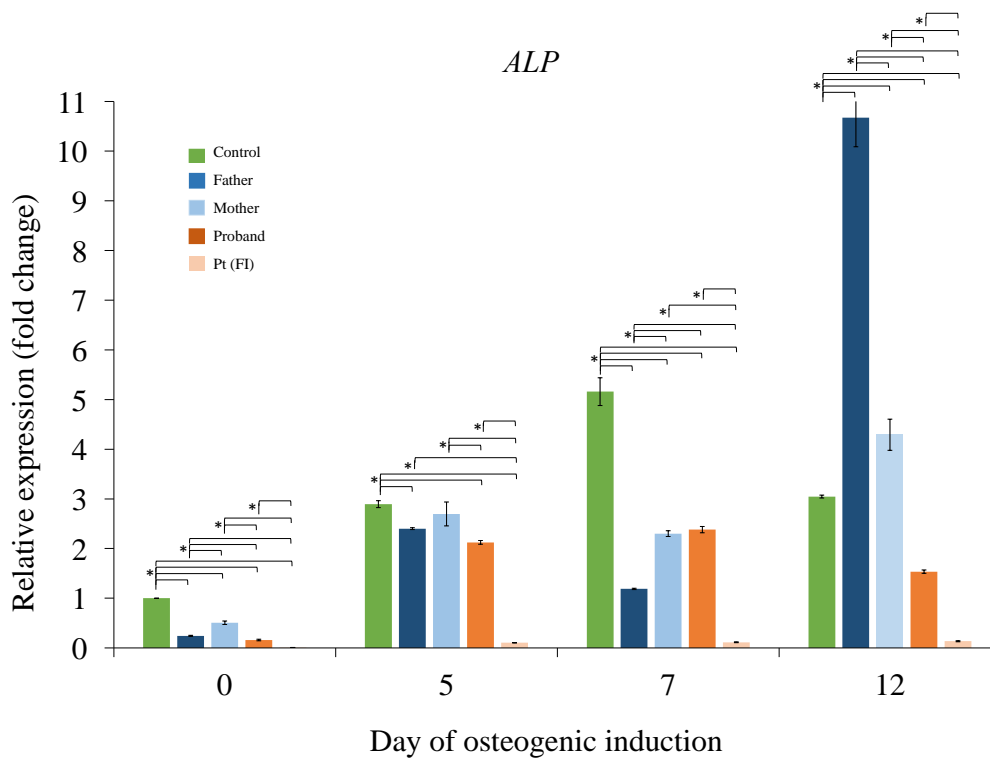


Figure 24 Expression of *ALP* gene. Level of ALP expression in ESC and patient iPSC-derived MSC during osteoblast differentiation at day 0, 5, 7, and 12 which was assayed by real-time PCR and showed as the relative expression in the fold of the control. The ESC-derived MSC was used as the control. * $p < 0.05$ compared to each other.

8.2 Mineralization assay

The mineralization assay of iPSC-derived MSC during osteoblast differentiation was performed by alizarin red staining at day 20 and 28. The ESC-derived MSC was used as the control. Alizarin red is the indicator of mineralized-like nodules and the positive staining was qualitative determination. Figure 25 shows calcium deposits produced by iPSC-derived MSC in each line. When compare with ESC-derived MSC, patient iPSC-derived MSC showed delay and low levels of calcium deposition during osteoblast differentiation. Calcium deposition was significantly low in pt (FII) iPSC-derived MSC compared with ESC, father, mother, and proband iPSC-derived MSC during osteoblast differentiation. This result indicated that *COL1A2* mutation in patients iPSC derived-MSC impaired osteoblast mineralization and maturation with downregulation of osteogenic genes.

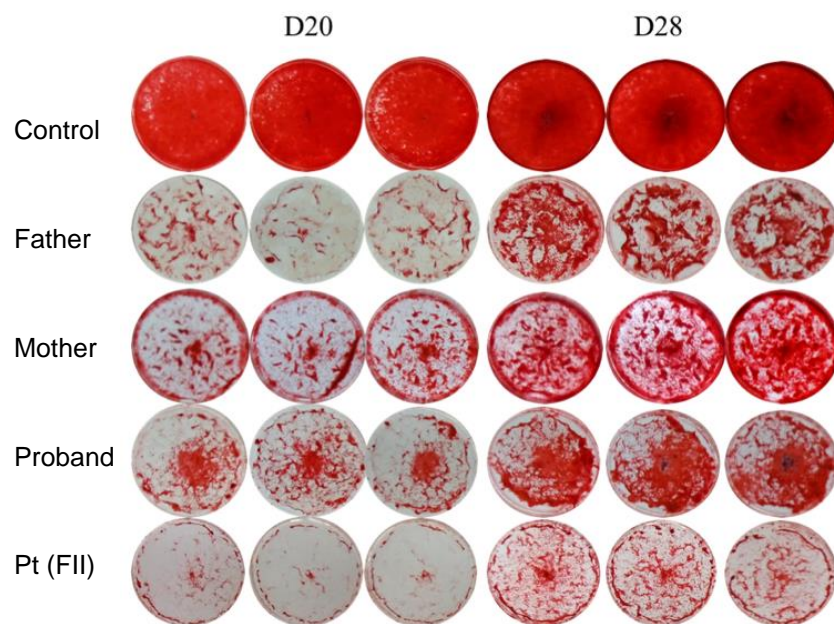


Figure 25 Calcium deposit during osteoblast differentiation. Calcium deposit at day 20 and 28 during osteoblast differentiation in ESC and patients iPSC-derived MSC was determined by alizarin red staining.

9. Investigation of biochemical substances involving mineralization

Osteocalcin, and osteopontin in culture medium of each iPSC-derived MSC were determined by ELISA assay at day 5, 7, and 12 after treated with osteogenic induction medium. The ESC-derived MSC was used as the control.

9.1 level of osteocalcin

Level of secreted osteocalcin in condition media was also determined by ELISA. The result showed that osteocalcin was not detected in proband and pt (FII) iPSC-derived MSC. While father and mother iPSC-derived MSC exhibited similar osteocalcin levels compared with ESC-derived MSC (Figure 26)

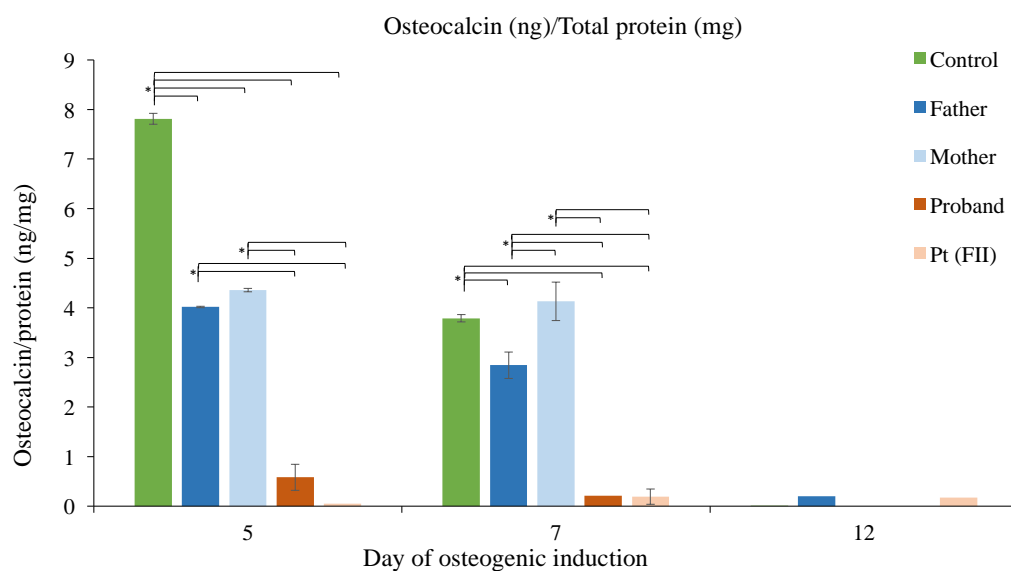


Figure 26 Level of extracellular osteocalcin. Level of osteocalcin in ESC and patient iPSC-derived MSC during osteoblast differentiation at day 5, 7, and 12 was assayed by ELISA and displayed as osteocalcin per total protein (ng/mg). The ESC-derived MSC was used as the control. * $p < 0.05$ compared to each other.

9.3 Level of osteopontin

It was found that osteopontin level showed the same pattern of expression as osteocalcin level. Osteopontin was not detected in proband and pt (FII) iPSC-derived MSC at day 5 and 7 whereas father and mother iPSC-derived MSC showed a lower level than ESC-derived MSC (Figure 27). In addition, all of sample did not exhibited osteopontin at day 12 (data not shown). The result demonstrated that osteopontin level was consistent with *SPP1* expression level in all iPSC-derived MSC during differentiation.

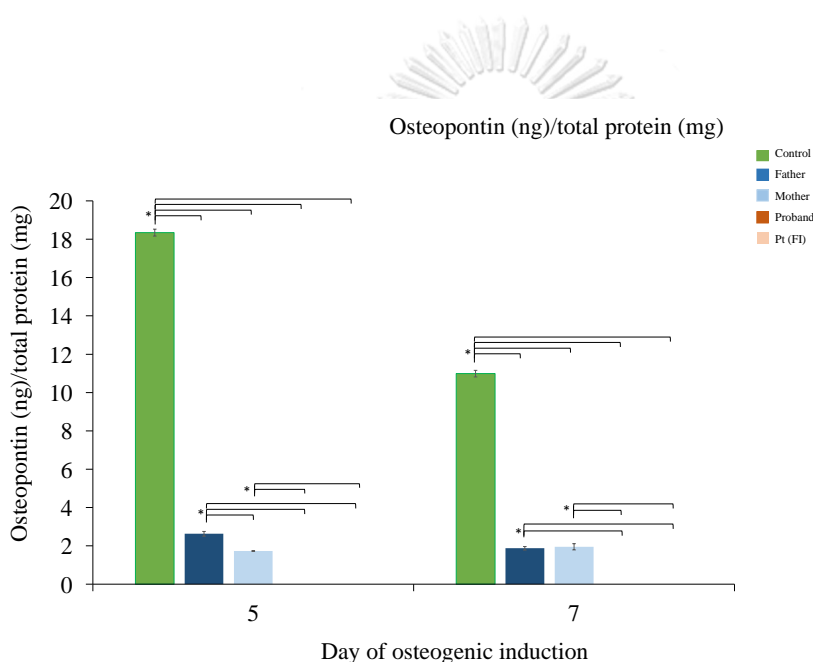


Figure 27 Level of extracellular osteopontin. Level of osteopontin in ESC and patient iPSC-derived MSC during osteoblast differentiation at day 5, 7, and 12 was assayed by ELISA and displayed as osteocalcin per total protein (ng/mg). The ESC-derived MSC was used as the control. * $p < 0.05$ compared to each other.

Discussion

Here, we established patient-specific iPSCs of a family which father and mother were DI patient with heterozygous *COL1A2* mutation and proband have OI and DI caused by homozygous *COL1A2* mutation to used as an in vitro system to screen for substances. The alpha 2(I) chain encoded by *COL1A2* gene is a major component of type I collagen in the bone (8, 27). The mutation in the *COL1A2* gene has been identified as the main cause of DI and OI. Normally, the *COL1A2* mutation is a cause of OI and inherited in a dominant manner (8). However, the parents of OI type III patient in the present study, who carry the heterozygous *COL1A2* mutation, do not show the OI phenotype. It could be indicated that not only mutation in *COL1A2* is a primary causative of clinical phenotype, but also the combination of modifier genes and/or environmental factors that affected the clinical phenotype. According to the previous reports about the discrepancies of genotype-phenotype correlation, this family provided the opportunity to investigate the pathogenesis of mono- and biallelic *COL1A2* mutation based on molecular phenotype by using the established patient-specific iPSCs as an in vitro system.

The generation of iPSC from OI fibroblast is enhanced by the use of human umbilical cord blood-derived serum (hUCS) in the fibroblast culture medium. Previous data demonstrate the benefit of hUCS in the culture of human foreskin fibroblast (46). The umbilical cord blood serum contained a high concentration of biologically active components and growth factors which are essential for cell proliferation and differentiation such as EGF and TGF- β (47). This could be explained that the transformation of dermal fibroblast into iPSC required more essential components and growth factors to drive the cell reprogramming.

After differentiation of iPSC into MSC, level of MSC marker expression was determined by flow cytometry. It was expected that the expression level of surface MSC marker should be higher than 95% (48-50). As shown in table 7, the level CD105 in pt (FII)-iPSC derived MSC was lower than 95%. These results are consistent with previous research (48). MSC with a low level of CD105 (~50%) exhibit the ability to differentiate toward the osteogenic lineage (48). The previous report demonstrates CD105 plays an important role in angiogenesis (48). It might be

suggested that a low level of CD105 in iPSC-derived MSC may not affect the osteogenic induction in the present study.

The present study showed that type I collagen of the trio were not be able to detect for the over modification by using SDS-urea PAGE, while that of pt (FII) showed abnormal electrophoretic migration resulted in a double band of 1 and 2 chain. It may have been because the mutation in *COL1A2* at a position near carboxy-terminal of type I collagen leads to a structural abnormality of type I collagen more than the mutation near amino terminal (51). Moreover, all of patient iPSCs-derived osteoblasts shows the lower level of procollagen I in both patient with OI and without OI and decreased the expression level of osteogenic markers including *OC*, *SPP1*, *ALP*, *COL1A1*, and *COL1A2* which resulted in impaired osteoblast differentiation and maturation. Subsequently, we found the differences in the level of extracellular osteocalcin and osteopontin between the patient with OI and without OI. This could be explained that the secretion of the mutated type I collagen can be reduced by a decreased rate of protein synthesis or induce ER stress due to cellular retention of misfolded type I collagen and/or degradation (2, 5). As for the calcium mineralization, all of the patient-iPSC-derived osteoblasts showed the delayed mineralization. According to Kim et al (2015), patient with Menkes disease, which had weakened bone matrix and low mineral density, Menkes-iPSC derived osteoblast showed downregulation of the osteoblast-specific genes and low levels of calcium deposition during osteoblast differentiation (52). It could be explained that impaired osteoblast differentiation may be caused by cell stress response due to the collection of misfolded procollagen in osteoblast(5). This report confirmed the impaired osteoblast differentiation is the major properties of bone disease. Our findings thus lend support that the established DI and OI-patient-specific iPSCs are able to use as an in vitro system to screen for biochemical substances which are able to improve OI osteoblasts' functions. The biochemical substance related to phenotype is osteocalcin and osteopontin which show lower expression level in a patient with OI than a patient without OI. The finding of the present study suggested that osteocalcin and osteopontin may act as modifier genes that amplify the severity bone defect resulting in OI in OI

patients who carry the same *COL1A2* mutation with father and mother of the proband. It could be suggested that osteocalcin and osteopontin may act as biochemical markers that may be useful for monitoring bone formation improvement in the clinical investigation of bone defect disease.

Osteocalcin and osteopontin are non-collagenous proteins (NCPs) which associated with regulating bone mineral. They are the major matrix component of the bone that controls the mineral size and bone matrix organization that involves the strength of bone (53, 54). Osteocalcin and osteopontin are produced during bone formation; therefore, impaired osteoblast differentiation may lead to a low level of these two components.

Osteopontin is expressed in a variety of human tissues including bone, dentin, cement, cartilage, and kidney (55) (56). Normally, osteopontin regulates crystal growth as well as crystal composition and act as basically functions as a nucleator of bone mineral. Beside, osteocalcin expanded mineral organic interaction by control hydroxyapatite crystal growth through the collagen fibril (47). The previous study demonstrated that the removal of both osteocalcin and osteopontin from the bone matrix of wild type mouse induces bone morphologies adaptation at the structural level including cortical area and length to maintain bone strength (53). It might be speculated that impaired osteoblast differentiation and maturation due to the induction of stress response by degradation and/or retention of misfolded type I collagen which leads to the low level of type I collagen synthesis, osteocalcin, and osteopontin could result in the defective bone structure of OI patients.

OI mouse models have been previously reported in several studies. In 2016, Mirigan et. al reported that *Coll1a2 (+/G610C)* mouse revealed osteoblast malfunction with converts osteoblast differentiation and function including low-level expression of *bglap* (5). However, the interspecies differences are the distinct disadvantage of animal cells and result in the extrapolation problematic (57). The *in vitro* system established from a human is a valuable tool with no interspecies differences which provide an opportunity to investigate the molecular and

cellular mechanisms of bone diseases including regulation of cell differentiation, synthesis, and secretion of matrix proteins, and drug pharmacokinetics (57).

The use of human OI osteoblast has been exhibited in several studies. Kaneto et. al (2016) showed significantly low expression of osteogenesis markers, including *BGLAP*, *COL1A1*, *MSX2*, *SPARC*, and *VDR* during osteoblast differentiation of MSC obtained from OI patients (4). On the other hand, Reich et. al (2015) demonstrated gain-of-function at osteoblast level which the expression of *ALP*, *IBSP*, *OC*, *OPN*, and the mineralization was increased but significantly decreased *COL1A1* transcripts in type V OI caused by *IFIMT5* mutation (58). However, the limited accessibility and long isolation procedures are the disadvantages of human osteoblast. The in vitro system established from the OI and DI patient-specific iPSC could be a powerful tool for using in the multi-propose for the development of bone disease treatment such as regenerative medicine and drug screening. According to the study of Deyle et. al in 2012, the study exhibit the combination between gene targeting and iPSC derivation isolated from OI patient were able to differentiate into osteoblast and produce normal collagen and bone in vivo that may be useful for OI treatment (59). In addition, targeting ER stress might offer a new therapeutic strategy to restore osteoblast's functions. Furthermore, the use of the level of osteocalcin and osteopontin as the potential marker according to the risk of bone fracture may benefit in improving the quality of life of the OI patient. As in the diagnosis of OI, the genetic determination of the OI causative gene may not the precision method due to the discrepancies of genotype-phenotype correlation. They might be the indicator to considered for the activity and occupy to according to the bone fracture risk

In summary, we established the trio-specific iPSC with the same genetic background to use as an in vitro system for exploring the biochemical substance which is able to improve OI osteoblasts' functions. Trio-specific iPSC displayed the molecular and cellular level that exhibited the impairment of the osteoblast differentiation and maturation. Osteocalcin and osteopontin level was different in DI patient with and without clinical OI. The association between clinical and quantitative defect of osteocalcin and osteopontin indicated that osteocalcin

and osteopontin may use as a surrogate marker to monitor bone fracture at the cellular level which may be developed to use for the diagnosis of OI. In addition, an in vitro system are sources of cell-based drug screening that provide the investigation of treatment for OI and bone fracture diseases in further study.



REFERENCES

1. Forlino A, Marini JC. Osteogenesis imperfecta. *Lancet*. 2016;387(10028):1657-71.
2. Bateman JF, Boot-Handford RP, Lamande SR. Genetic diseases of connective tissues: cellular and extracellular effects of ECM mutations. *Nat Rev Genet*. 2009;10(3):173-83.
3. Ohba S, Chung UI, Tei Y. [Osteoblast differentiation induced by BMP signaling and Runx2 through Cbfb regulation]. *Nihon Rinsho*. 2007;65 Suppl 9:71-4.
4. Kaneto CM, Lima PS, Zanette DL, Oliveira TY, de Assis Pereira F, Lorenzi JC, et al. Osteoblastic differentiation of bone marrow mesenchymal stromal cells in Bruck Syndrome. *BMC Med Genet*. 2016;17(1):38.
5. Mirigian LS, Makareeva E, Mertz EL, Omari S, Roberts-Pilgrim AM, Oestreich AK, et al. Osteoblast Malfunction Caused by Cell Stress Response to Procollagen Misfolding in alpha2(I)-G610C Mouse Model of Osteogenesis Imperfecta. *J Bone Miner Res*. 2016;31(8):1608-16.
6. De Paepe A, Nuytinck L, Raes M, Fryns J-P. Homozygosity by descent for a COL1A2 mutation in two sibs with severe osteogenesis imperfecta and mild clinical expression in the heterozygotes. *Human genetics*. 1997;99(4):478-83.
7. Costantini A, Tournis S, Kampe A, Ul Ain N, Taylan F, Doulgeraki A, et al. Autosomal Recessive Osteogenesis Imperfecta Caused by a Novel Homozygous COL1A2 Mutation. *Calcif Tissue Int*. 2018.
8. Marini JC, Forlino A, Bachinger HP, Bishop NJ, Byers PH, Paepe A, et al. Osteogenesis imperfecta. *Nat Rev Dis Primers*. 2017;3:17052.
9. DW R. Osteogenesis imperfecta. *Principles of bone biology Academic Press*; 2002. p. 1177-93.
10. Forlino A, Cabral WA, Barnes AM, Marini JC. New perspectives on osteogenesis imperfecta. *Nat Rev Endocrinol*. 2011;7(9):540-57.
11. consortium Bbd. Disorder definitions [Available from: <https://www.rarediseasesnetwork.org/cms/bbd/Healthcare-Professionals/Disorder-Definitions>].
12. Rauch F, Lalic L, Roughley P, Glorieux FH. Genotype-phenotype correlations in nonlethal osteogenesis imperfecta caused by mutations in the helical domain of collagen type I. *Eur J Hum Genet*. 2010;18(6):642-7.

13. Lindahl K, Astrom E, Rubin CJ, Grigelioniene G, Malmgren B, Ljunggren O, et al. Genetic epidemiology, prevalence, and genotype-phenotype correlations in the Swedish population with osteogenesis imperfecta. *Eur J Hum Genet.* 2015;23(8):1042-50.
14. Maioli M, Gnoli M, Boarini M, Tremosini M, Zambrano A, Pedrini E, et al. Genotype-phenotype correlation study in 364 osteogenesis imperfecta Italian patients. *Eur J Hum Genet.* 2019.
15. Boskey AL. Bone composition: relationship to bone fragility and antiosteoporotic drug effects. *Bonekey Rep.* 2013;2:447.
16. Kini U NB. *Physiology of Bone Formation, Remodeling, and Metabolism. Radionuclide and hybrid bone imaging.* Berlin, Heidelberg.: Springer; 2012. p. 29-57.
17. Florencio-Silva R, Sasso GR, Sasso-Cerri E, Simoes MJ, Cerri PS. Biology of Bone Tissue: Structure, Function, and Factors That Influence Bone Cells. *Biomed Res Int.* 2015;2015:421746.
18. Miron RJ, Zhang YF. Osteoinduction: a review of old concepts with new standards. *J Dent Res.* 2012;91(8):736-44.
19. Orimo H. The mechanism of mineralization and the role of alkaline phosphatase in health and disease. *J Nippon Med Sch.* 2010;77(1):4-12.
20. Ishida M, Amano S. Osteocalcin fragment in bone matrix enhances osteoclast maturation at a late stage of osteoclast differentiation. *J Bone Miner Metab.* 2004;22(5):415-29.
21. Cremers S, Garnero P, Seibel MJ. Biochemical markers of bone metabolism. *Principles of Bone Biology (Third Edition): Elsevier;* 2008. p. 1857-81.
22. Patti A, Gennari L, Merlotti D, Dotta F, Nuti R. Endocrine actions of osteocalcin. *International journal of endocrinology.* 2013;2013.
23. Jagtap VR, Ganu JV. SERUM OSTEOCALCIN: A SPECIFIC MARKER FOR BONE FORMATION IN POSTMENOPAUSALOSTEOPOROSIS. *Bone.* 2011;2:5.
24. Zurick KM, Qin C, Bernardis MT. Mineralization induction effects of osteopontin, bone sialoprotein, and dentin phosphoprotein on a biomimetic collagen substrate. *Journal of Biomedical Materials Research Part A.* 2013;101(6):1571-81.
25. Sapir-Koren R, Livshits G. Bone mineralization and regulation of phosphate homeostasis. *IBMS BoneKEy.* 2011;8(6):286-300.
26. Malaval L, Wade-Guéye NM, Boudiffa M, Fei J, Zirngibl R, Chen F, et al. Bone sialoprotein plays a functional role in bone formation and osteoclastogenesis. *Journal of*

Experimental Medicine. 2008;205(5):1145-53.

27. Canty EG, Kadler KE. Procollagen trafficking, processing and fibrillogenesis. *J Cell Sci.* 2005;118(Pt 7):1341-53.
28. Greenblatt MB, Tsai JN, Wein MN. Bone Turnover Markers in the Diagnosis and Monitoring of Metabolic Bone Disease. *Clin Chem.* 2017;63(2):464-74.
29. Eyre DR, Paz MA, Gallop PM. Cross-linking in collagen and elastin. *Annu Rev Biochem.* 1984;53:717-48.
30. Astrom E, Magnusson P, Eksborg S, Soderhall S. Biochemical bone markers in the assessment and pamidronate treatment of children and adolescents with osteogenesis imperfecta. *Acta Paediatr.* 2010;99(12):1834-40.
31. Viguet-Carrin S, Garnero P, Delmas PD. The role of collagen in bone strength. *Osteoporos Int.* 2006;17(3):319-36.
32. Marie PJ, Hay E, Saidak Z. Integrin and cadherin signaling in bone: role and potential therapeutic targets. *Trends Endocrinol Metab.* 2014;25(11):567-75.
33. Xiao G, Jiang D, Gopalakrishnan R, Franceschi RT. Fibroblast growth factor 2 induction of the osteocalcin gene requires MAPK activity and phosphorylation of the osteoblast transcription factor, Cbfa1/Runx2. *J Biol Chem.* 2002;277(39):36181-7.
34. Xiao G, Gopalakrishnan R, Jiang D, Reith E, Benson MD, Franceschi RT. Bone morphogenetic proteins, extracellular matrix, and mitogen-activated protein kinase signaling pathways are required for osteoblast-specific gene expression and differentiation in MC3T3-E1 cells. *J Bone Miner Res.* 2002;17(1):101-10.
35. Huang RL, Yuan Y, Tu J, Zou GM, Li Q. Opposing TNF-alpha/IL-1beta- and BMP-2-activated MAPK signaling pathways converge on Runx2 to regulate BMP-2-induced osteoblastic differentiation. *Cell Death Dis.* 2014;5:e1187.
36. Phimphilai M, Zhao Z, Boules H, Roca H, Franceschi RT. BMP signaling is required for RUNX2-dependent induction of the osteoblast phenotype. *J Bone Miner Res.* 2006;21(4):637-46.
37. Dong M, Jiao G, Liu H, Wu W, Li S, Wang Q, et al. Biological Silicon Stimulates Collagen Type 1 and Osteocalcin Synthesis in Human Osteoblast-Like Cells Through the BMP-2/Smad/RUNX2 Signaling Pathway. *Biol Trace Elem Res.* 2016;173(2):306-15.
38. Sun X, Xie Z, Ma Y, Pan X, Wang J, Chen Z, et al. TGF-beta inhibits osteogenesis by

upregulating the expression of ubiquitin ligase SMURF1 via MAPK-ERK signaling. *J Cell Physiol.* 2018;233(1):596-606.

39. Grafe I, Yang T, Alexander S, Homan EP, Lietman C, Jiang MM, et al. Excessive transforming growth factor-beta signaling is a common mechanism in osteogenesis imperfecta. *Nat Med.* 2014;20(6):670-5.

40. Sangsin A, Srichomthong C, Pongpanich M, Suphapeetiporn K, Shotelersuk V. Short stature, platyspondyly, hip dysplasia, and retinal detachment: an atypical type II collagenopathy caused by a novel mutation in the C-propeptide region of COL2A1: a case report. *BMC Med Genet.* 2016;17(1):96.

41. Pruksananonda K, Rungsiwiwut R, Numchaisrika P, Ahnonkitpanit V, Isarasena N, Virutamasen P. Eighteen-year cryopreservation does not negatively affect the pluripotency of human embryos: evidence from embryonic stem cell derivation. 2012;1(4):166-73.

42. Park I-H, Zhao R, West JA, Yabuuchi A, Huo H, Ince TA, et al. Reprogramming of human somatic cells to pluripotency with defined factors. *Nature.* 2008;451(7175):141.

43. Page RL, Ambady S, Holmes WF, Vilner L, Kole D, Kashpur O, et al. Induction of stem cell gene expression in adult human fibroblasts without transgenes. *Cloning and stem cells.* 2009;11(3):417-26.

44. Cabral WA, Perdivara I, Weis M, Terajima M, Blissett AR, Chang W, et al. Abnormal type I collagen post-translational modification and crosslinking in a cyclophilin B KO mouse model of recessive osteogenesis imperfecta. *PLoS Genet.* 2014;10(6):e1004465.

45. Chen YS, Pelekanos RA, Ellis RL, Horne R, Wolvetang EJ, Fisk NM. Small molecule mesengenic induction of human induced pluripotent stem cells to generate mesenchymal stem/stromal cells. *Stem cells translational medicine.* 2012;1(2):83-95.

46. Rungsiwiwut R, Ingrungruenglert P, Numchaisrika P, Virutamasen P, Phermthai T, Pruksananonda K. Human Umbilical Cord Blood-Derived Serum for Culturing the Supportive Feeder Cells of Human Pluripotent Stem Cell Lines. *Stem Cells Int.* 2016;2016:4626048.

47. Poundarik AA, Boskey A, Gundberg C, Vashishth D. Biomolecular regulation, composition and nanoarchitecture of bone mineral. *Sci Rep.* 2018;8(1):1191.

48. Duff SE, Li C, Garland JM, Kumar S. CD105 is important for angiogenesis: evidence and potential applications. *FASEB J.* 2003;17(9):984-92.

49. Dominici M, Le Blanc K, Mueller I, Slaper-Cortenbach I, Marini F, Krause D, et al. Minimal criteria for defining multipotent mesenchymal stromal cells. The International Society for Cellular Therapy position statement. *Cytotherapy*. 2006;8(4):315-7.
50. Moraes DA, Sibov TT, Pavon LF, Alvim PQ, Bonadio RS, Da Silva JR, et al. A reduction in CD90 (THY-1) expression results in increased differentiation of mesenchymal stromal cells. *Stem Cell Res Ther*. 2016;7(1):97.
51. Cabral WA, Milgrom S, Letocha AD, Moriarty E, Marini JC. Biochemical screening of type I collagen in osteogenesis imperfecta: detection of glycine substitutions in the amino end of the alpha chains requires supplementation by molecular analysis. *J Med Genet*. 2006;43(8):685-90.
52. Kim D, Choi J, Han KM, Lee BH, Choi JH, Yoo HW, et al. Impaired osteogenesis in Menkes disease-derived induced pluripotent stem cells. *Stem Cell Res Ther*. 2015;6:160.
53. Bailey S, Karsenty G, Gundberg C, Vashishth D. Osteocalcin and osteopontin influence bone morphology and mechanical properties. *Ann N Y Acad Sci*. 2017;1409(1):79-84.
54. Tsao YT, Huang YJ, Wu HH, Liu YA, Liu YS, Lee OK. Osteocalcin Mediates Biom mineralization during Osteogenic Maturation in Human Mesenchymal Stromal Cells. *Int J Mol Sci*. 2017;18(1).
55. Nikel O, Poundarik AA, Bailey S, Vashishth D. Structural role of osteocalcin and osteopontin in energy dissipation in bone. *J Biomech*. 2018;80:45-52.
56. Sodek J, Ganss B, McKee MD. Osteopontin. *Crit Rev Oral Biol Med*. 2000;11(3):279-303.
57. Czekanska EM, Stoddart MJ, Richards RG, Hayes JS. In search of an osteoblast cell model for in vitro research. *Eur Cell Mater*. 2012;24:1-17.
58. Reich A, Bae AS, Barnes AM, Cabral WA, Hinek A, Stimec J, et al. Type V OI primary osteoblasts display increased mineralization despite decreased COL1A1 expression. *J Clin Endocrinol Metab*. 2015;100(2):E325-32.
59. Deyle DR, Khan IF, Ren G, Wang PR, Kho J, Schwarze U, et al. Normal collagen and bone production by gene-targeted human osteogenesis imperfecta iPSCs. *Mol Ther*. 2012;20(1):204-13.

Appendix

Table 9 Raw data of total protein quantitated by BCA assay

Total prot. (mg/ml)	Day of osteogenic induction	
	D5	D7
Control	0.6934	1.2284
Father	1.3498	1.6152
Mother	1.3179	1.3227
Proband	1.4456	1.6720
Pt (FII)	1.8550	1.6611

Table 10 Level of osteocalcin/total protein (ng/mg)

Mean OCN/total protein (ng/mg)	Day of osteogenic induction			SD	Day of osteogenic induction	
	D5	D7	D12		D5	D7
Control	7.8128	3.7902	0.0002	Control	0.1091	0.0737
Father	4.01725	2.8424	0.2015	Father	0.0141	0.2653
Mother	4.3583	4.1316		Mother	0.0333	0.3881
Proband	0.5821	0.2111		Proband	0.2627	0.2986
Pt (FII)	0.0488	0.1914	0.1739	Pt (FII)	0.0690	0.1541

Table 11 Level of osteopontin/total protein (ng/mg)

Mean OPN/total protein (ng/mg)	Day of osteogenic induction		SD	Day of osteogenic induction	
	D5	D7		D5	D7
Control	18.2170	10.9855	Control	0.1802	0.1716
Father	2.5416	1.8722	Father	0.1234	0.0918
Mother	1.7261	1.9508	Mother	0.0059	0.1613
Proband	0	0	Proband	-	-
Pt (FII)	0	0	Pt (FII)	-	-

Table 12 Level of PIP/total protein (ng/mg)

PIP/ total protein (ng/mg)	D0	D5	D7	D12
Control	1	1.1542	1.1666	1.1130
Father	0.9384	1.0154	0.9031	1.1041
Mother	0.7330	1.1097	0.5816	0.7037
Proband	1.0965	1.3231	0.7606	1.1804
Pt (FII)	0.6587	1.0082	0.9394	0.9814

Table 13 Raw quantitative qPCR cycle threshold for osteogenic genes and housekeeping gene

Sample/Ct	<i>OC 5 ul</i>	<i>GAPDH 1 ul for OC 5 ul</i>	<i>SPP1</i>	<i>COL1A1</i>	<i>COL1A2</i>	<i>ALP</i>	<i>GAPDH</i>
Control D0	31.31682014	16.44060707	21.4278052	21.1088047	21.14299965	29.89544106	16.99848175
Control D0	31.30241966	16.20158195	21.4623085	21.0446167	21.07208252	29.97288322	16.98138618
Control D0	30.77369118	16.27684021	21.4197631	20.92035103	21.03198814	29.91677094	16.84869766
Control D5	30.89522934	16.66351891	20.3874878	22.32289505	21.9233799	28.88682175	17.54455757
Control D5	30.97098732	16.73364258	20.36859092	22.28121758	22.00527382	28.87489891	17.40818977
Control D5	30.65107918	16.84698677	20.37521273	22.33669281	21.99782562	28.94097328	17.39369583
Control D7	30.60419083	16.6957016	20.5980379	19.99759102	20.53678322	27.79461098	17.25885201
Control D7	30.9482975	16.76118279	20.61011405	20.0628376	20.60148048	27.94641304	17.29929161
Control D7	30.77952385	16.87732315	20.60501478	20.05534935	20.58047485	27.89811897	17.22261047
Control D12	33.55577087	16.2566452	21.92662334	23.17995262	22.8750267	28.24902153	16.83119011
Control D12	34.38610077	16.46693039	21.90457915	23.04024696	22.8366375	28.1730938	16.78721428
Control D12	34.50322723	16.64496422	21.97294626	23.14412117	22.88072205	28.15080261	16.81970215
Father D0	30.44112587	15.67818546	25.09210821	20.32618141	21.43557358	31.21572113	16.16264915
Father D0	30.19643021	15.65544319	25.07644973	20.27277184	21.37050438	31.1468277	16.19356918
Father D0	30.52492714	15.67911243	25.13277043	20.2263813	21.37639999	31.27460861	16.18441582
Father D5	30.75793076	15.66873074	26.32006892	20.51243019	22.02379227	30.68136215	18.93015289
Father D5	30.97766685	15.65490341	26.4904197	20.53539276	22.18344116	30.69114304	18.99113083
Father D5	30.63820839	15.72994804	26.32016931	20.51483154	22.09586906	30.70410347	18.99084091
Father D7	31.8327961	16.13928986	25.09337791	19.79194832	20.36692047	29.12820816	16.36048698
Father D7	30.94354248	15.98139286	25.08255845	19.76371384	20.35442924	29.14621353	16.45388603
Father D7	30.97233582	15.94725132	25.06936875	19.72949028	20.36962318	29.15821457	
Father D12	30.83988571	15.57979679	26.74101482	20.35100174	23.20981979	29.4125061	19.93281937
Father D12	30.36603546	15.55569363	26.6731292	20.4003067	23.19898796	29.57068062	19.90919685
Father D12	30.47776222	15.61633015	26.77910974	20.47536087	23.31939316	29.49164963	
Mother D0	29.11103058	16.70669365	27.04958144	21.07868385	21.01442719	31.46177864	17.36629868
Mother D0	28.96626663	16.8831234	27.02325036	21.07738495	21.08502007	31.50323868	17.49996948
Mother D0	29.4023304	16.93650246	26.97069603	21.06168365	21.07706261	31.31567383	17.50490189
Mother D5	29.14210129	17.15244675	31.23926977	21.01425171	21.61157036	29.81721306	18.23405838
Mother D5	29.16156387	17.36607742	31.44188373	20.99828529	21.64253235	29.93262482	18.39823151
Mother D5	29.14262199	17.36041641	31.46246302	20.98741722	21.6183567	30.07576561	18.52000618
Mother D7	28.54336357	16.97578621	26.60670476	20.88548851	21.40636444	29.69747353	17.89124489
Mother D7	28.2767868	17.14600563	26.59190514	20.83184052	21.45050621	29.62583351	17.84985542
Mother D7	28.6808033	17.32948494	26.57636936	20.82902336	21.44955444	29.64726639	17.88029671
Mother D12	28.41606903	16.70181465	25.76871876	22.22640419	23.4954071	31.25734901	20.48412323
Mother D12	28.66456795	16.75892067	25.74588263	22.21664238	23.5436554	31.46630096	20.48349953
Mother D12	28.74987411	16.66390228	25.76336294	22.34346199	23.69923592	31.37859344	20.47575951

Table 13 Raw quantitative qPCR cycle threshold for osteogenic genes and housekeeping gene (*continue*)

Sample/Ct	<i>OC 5 ul</i>	<i>GAPDH 1 ul for OC 5 ul</i>	<i>SPP1</i>	<i>COL1A1</i>	<i>COL1A2</i>	<i>ALP</i>	<i>GAPDH</i>
Proband D0	31.32850075	16.10756683	26.55741113	22.53212929	23.18955803	32.56003571	16.74801064
Proband D0	32.11735535	16.15361977	26.49378823	22.46266747	23.04724312	32.34238815	16.81300735
Proband D0	34.0015564	16.27846909	26.4371106	22.3838253	22.9372406	32.29121017	16.7167263
Proband D5	30.86429977	16.08774185	25.3022958	19.95282364	20.19646454	28.34306908	16.39938736
Proband D5	31.10403442	15.96309948	25.28152317	19.89721298	20.27042198	28.3941021	16.64151573
Proband D5	30.66976547	16.17696762	25.29383728	19.8836937	20.16973686	28.36392212	16.36513901
Proband D7	32.34417725	15.9447937	26.95583507	19.8974781	20.730793	28.38461876	16.64538002
Proband D7	32.61791611	15.94865227	26.93041491	19.8745575	20.72820663	28.3310833	16.58527184
Proband D7	31.01556396	16.13886642	26.8884142	19.8715477	20.76652527	28.30955505	16.59406281
Proband D12	31.47655869	15.32667637	27.72333655	20.11435318	21.27851486	28.50730324	16.16699028
Proband D12	31.99118423	15.41655827	27.61088849	20.09599686	21.28232384	28.46119499	16.16133118
Proband D12	31.47472954	15.40990448	27.55514037	20.14380646	21.33580399	28.4481945	15.98789978
Pt (FII) D0	32.39478302	15.48741341	28.51134666	20.43876457	21.05908203	35.96880341	16.00048828
Pt (FII) D0	30.95589828	15.58289337	28.4573832	20.22060585	20.90559578	35.77536774	16.06291962
Pt (FII) D0	31.81279755	15.74307823	28.5501666	20.20988655	20.88467598	35.69887924	15.88813305
Pt (FII) D5	32.52655792	16.34083939	29.26560824	20.36461258	21.1645031	32.84734344	16.65394211
Pt (FII) D5	32.18431854	16.42716026	29.42446658	20.29810905	21.06567955	32.99934387	16.65834999
Pt (FII) D5	32.31602859	16.39097786	29.55170124	20.29084778	21.00919342	32.90507507	16.67070389
Pt (FII) D7	30.95844841	15.92950058	28.81778472	19.7085228	20.16411591	32.44570923	16.24432182
Pt (FII) D7	30.49921227	15.86396599	28.87856705	19.70246506	20.15017319	32.2782135	16.28464508
Pt (FII) D7	31.09060669	15.94376659	28.94858496	19.70059013	20.19499207	32.46475983	
Pt (FII) D12	29.92141724	15.86458492	27.80970449	20.83751869	21.28669357	32.28078842	16.29437447
Pt (FII) D12	29.59313583	15.90862656	27.71352839	20.86255646	21.35473824	32.06954956	16.21094322
Pt (FII) D12	30.27396202	15.87395954	27.68183033	20.85981178	21.27136803	32.09919357	16.30047989

VITA

NAME	Wandee Udomchaiprasertkul
DATE OF BIRTH	15 May 1980
PLACE OF BIRTH	Chonburi
HOME ADDRESS	3/10 Moo.3 Soi. Success Surasak Sriracha Chonburi



จุฬาลงกรณ์มหาวิทยาลัย
CHULALONGKORN UNIVERSITY